Unpaved roads' surface evaluation using unmanned aerial vehicle and deep learning segmentation

by

Luana Lopes Amaral Loures

A thesis
presented to Lakehead University
in fulfillment of the
thesis requirement of the degree of
Master of Science

Thunder Bay, Ontario, Canada, 2021

Author’s Declaration

I hereby declare that I am the sole author of the thesis. This is a true copy of the thesis, including any required final revisions, as accepted by my examiners.

I understand that my thesis may be made electronically available to the public.

Abstract

Unpaved roads have a significant role in Canada's transportation and service activities, accounting for close to 60% of Canada's total public road networks. Furthermore, they connect agricultural, mining, recreational areas, and small communities to the nearby towns and businesses. An effective maintenance program for a network of unpaved roads requires a detailed assessment of the road surface's condition, and such assessment is usually made by visual inspections which can be time-consuming and error prone. The main part of these evaluations aims to identify distresses on the road surface, such as washboarding (corrugation), potholes, and rutting. Many research studies have developed methods to automate condition assessment of asphalt roads by combining machine learning algorithms and low-cost unmanned aerial vehicles (UAV), but the research on the automated assessment of unpaved roads is very limited. A system has been developed in this study to automate the assessment of unpaved roads by coupling computer vision methods, namely deep convolutional neural networks, and UAV-based imaging. This automated system could be used as an alternative method to reduce the need for human effort and possible manual errors, and therefore improve road maintenance programs in remote areas. The performance of the proposed method was evaluated using different test settings, and despite having some challenges, such as false positives, it showed promising outcomes that can contribute to the proposed purpose of this research. This proposed method has a potential for further improvement and the findings can be used as a basis for similar studies.

Acknowledgments

Over the past year as a Master's student at Lakehead University, I have received support from many people that were crucial for achieving success during my journey, in many distinct ways. First and foremost, I would like to express my deepest appreciation to my supervisor, Prof. Ehsan Rezazadeh Azar, for his support, and encouragement. I have learned much through his teaching. He has always been thoughtful and helpful, especially when it comes to doubts or suggestions towards the research. I could not reach this stage without his supervision. It is such an honour to be his student.

Especially, I would like to appreciate my family, my mother (Elivane Lopes de Oliveira), who has taught me to be brave and face challenges with courage. My father (Marcos Antonio Loures do Amaral), who has served me as an example of strength and persistence. My sister (Lara Lopes Amaral Loures), for always give me support and tender words whenever I needed them most, my grandmother (Rita Lopes de Oliveira), who is my greatest representation of love and compassion. I also would like to offer special thanks to my great grandmother (Maria Antonia Mendanha), who, although no longer with us, continues to inspire by her example of strength and tenderness throughout her journey as our family matriarch.

At last, but not least, I would also like to thank my husband (Caio Belo Magalhaes), for having believed and trusted me in the pursuit of my dreams. Also, my mother-in-law (Wilma Lylian Belo Castilho), who has offered all the support and encouragement, and for having welcomed me into her family with so much love and affection.

Table of Contents

List of Figures

List of Tables

Nomenclature/List of Acronyms

AC	Alternating Current
ANN	Artificial Neural Networks
APL	Longitudinal Profile Analyzer
ASCE	American Society of Civil Engineers
ASTM	American Society for Testing and Materials
CAR	Canadian Aviation Regulations
CIA	Central Intelligence Agency
CMOS	Complementary Metal Oxide Semiconductor
CNN	Convolutional Neural Networks
CPU	Central Processing Unit
DCNN	Deep Convolutional Neural Network
DDR4	Double Data Rate 4
DJI	Da-Jiang Innovations
DSLR	Digital Single-lens Reflex
FN	False Negative
FP	False Positive
GB	Gigabyte
GCCRRM	Guidelines for Conducting and Calibrating Road Roughness Measurements
GCS	Ground Control Station
GDDR6	Graphics Double Data Rate
GHz	Gigahertz
GPU	Graphics Processing Unit
GTX	Giga Texel Shader eXtreme
ICAICTA	International Conference on Advanced Informatics: Concept Theory and Applications
ICIEA	International Conference on Industrial Engineering and Applications
ICLR	International Conference on Learning Representations
ICUAS	International Conference on Unmanned Aircraft Systems
IEEE	Institute of Electrical and Electronics Engineers
IOU	Intersection Over Union
IPT	Image Processing Techniques
IRI	International Roughness Index
IRRE	International Road Roughness Experiment

JPEG	Joint Photographic Experts Group
MB	Megabyte
MDEP	Maine Department of Environmental Protection
MP	Megapixels
PASER	Pavement Surface Evaluation and Rating
PAVER	Pavement Management Database Software
PMS	Pavement Management System
RAM	Random Access Memory
ReLU	Rectified Linear Unit
RTRRMS	Response-Type Road Roughness Measurement Systems
TP	True Positive
UAV	Unmanned Aerial Vehicle

Chapter 1: Introduction

1.1 Background and research motivation

Unpaved roads play an indispensable role in the road transportation system of many countries, especially in the countries with large territories, such as Canada, The United States, and Brazil. The importance of these roads is even more evident in the regions where scattered communities, farming, forestry, and industrial activities are present. In Canada, unpaved roads account for 60% of the total length of its public road network (Transport Canada 2018), while in Brazil it accounts for 88% of the total road network, and in the United States, the unpaved roads make up about 35% of the country's total road network (CIA 2021).

It is important to mention that unpaved roads play an essential role in the social and economical prosperity of remote regions, such as Indigenous communities, agricultural, mining, and recreational areas (e.g., provincial parks and conservation areas), which connect those communities to the nearby towns and businesses. Some of the unpaved roads connect farms to the closest cities, making them high-traffic roads in seasonal times.

Given the importance of unpaved roads in the socio-economic growth of remote communities, it is necessary to monitor the deterioration of these infrastructures due to various factors, including high levels of traffic load (e.g., used by heavy forestry or farming equipment), road structural design (for example, road crown and drainage system), weather and precipitation conditions, and the properties of the road surface materials. The road surface condition may affect vehicle operating costs by more than 50% (such as fuel consumption, and tire and maintenance costs), and it also affects the ride quality at a significant level (Archondo-Callao

2004). These items highlight the importance of evaluating unpaved road conditions to maintain these infrastructure assets at an acceptable level of service.

The surface deteriorations in unpaved roads can manifest in several physical forms, such as potholes, ripples (also known as washboarding or corrugations), rutting, and loose aggregates. There are various methods to assess unpaved roads conditions, but two methods are widely used: physical measurements of the irregularities on the longitudinal profile of a road, such as the International Roughness Index (IRI) method, and qualitative and quantitative visual assessment of the condition of unpaved roads, such as the methods proposed for civil roads (Eaton et al. 1989; Walker 1991).

The methods for physical measurement of the longitudinal profiles of the roads are effective and accurate ways to measure the road surface condition; however, they require special and expensive vehicles equipped with on-board sensors and laser profilers. But due to the limited budget and lack of resources, the visual methods are more common for the assessment of unpaved roads. Nevertheless, the visual assessment methods can run into some barriers, such as the subjectivity of the assessments and the amount of labor work and time required to perform such assessments (Saeed et al., 2020).

To address the subjective and demanding nature of manual road condition assessments, many research projects have developed methods to improve the automation level of road condition evaluation (for both paved and unpaved roads). Different data collection and processing methods, such as computer vision algorithms, vertical acceleration data processing, and 3D laser scanning, have been used to develop automated condition assessment systems (Saeed et al. 2020; Sattar et al. 2018).

UAVs are promising imaging platforms for inspecting unpaved roads because they can be operated at a relatively low cost and their operation in the sparsely populated areas is generally

not restricted by the flight restrictions that exist in many urban areas (Transport Canada 2019, 2020). Therefore, they can be a reliable tool to enhance the automation level of the road condition assessment processes, namely when they are coupled with computer vision-based methods.

Computer vision methods use image processing and machine learning algorithms to detect different road surface defects in the road images or video frames, which can provide a cost-effective solution for the assessment of the road surfaces (Saeed et al. 2020; Sattar et al. 2018). There are several studies on the application of such assessment methods on asphalt and concrete roads (Cao et al. 2020; Harikrishnan and Gopi 2017); however, only a small number of research projects focused on unpaved roads (Saeed et al. 2020). For example, there are a few research efforts that used computer vision algorithms for segmentation of the unpaved roads in images (Pereira et al. 2018) and detection of road surface damages (Nasiruddin Khilji et al. 2021; Dobson et al. 2013; Zhang and Elaksher 2012).

Due to significant advances in high-performance computing systems (such as CPU, GPU, and RAM) at reasonable costs, computer vision-based methods have achieved considerable attention in the past decade (Sahari Moghaddam et al., 2020). Moreover, incremental improvement of computer vision algorithms has encouraged the use of these methods for road condition assessment. For example, an obvious pattern has emerged since 2016, when most research projects switched to deep learning-based methods to detect defects.

Before deep learning, computer vision-based methods generally applied preprocessing filters to improve image lighting conditions and remove visual noises, and then extracted certain features (such as edges and histograms) to detect defects (Doycheva et al., 2016; Koch et al., 2015; Radopoulou and Brilakis, 2015). However, the Deep Convolutional Neural Network (DCNN) models provide an end-to-end method with better performance in detecting road

defects under different lighting conditions and visual noises. Several studies have investigated different DCNN models for detecting a single type of road defect, such as cracks (Liu et al. 2020; Li et al. 2020; Pan et al. 2018) and potholes (Pei et al. 2021; Ye et al. 2019). Most of these research efforts, however, focused on the paved roads (mostly asphalt roads) and the research on the application of DCNN-based methods for assessment of the unpaved roads is very limited; therefore, this research employs DCNN-based models to detect main defects on the unpaved road surfaces, including potholes, rutting, and washboarding, in the video frames captured by an UAV.

1.2 Research objectives

The aim of this research is to conduct a study on automated assessment of the unpaved roads. A system is developed by integration of methods from computer vision and machine learning (namely deep convolutional neural networks), infrastructure condition monitoring, and unmanned aerial systems to process UAV-captured images and identify distresses on the unpaved road surfaces.

The use of UAVs can increase the automation level and improve time savings of the condition assessment of these road networks compared to the conventional methods, which require extensive field observation by professionals to evaluate and classify these infrastructure assets. These manual methods are time consuming and require intense work and may present some safety concerns, especially due to the traffic flow.

Automating the road condition assessment process, such as automated detection of distresses on images, presents a valuable alternative for condition assessment. Therefore, this research aims to employ and assess the performance of different DCNN models in the segmentation of

the road surface and detection of three main defects, including potholes, washboarding, and rutting, on the identified surface of unpaved roads.

1.3 Research methods

This research proposes a system composed of UAV-based imaging for data collection and deep learning for distress recognition on the unpaved road surfaces. The collected data included UAV-captured videos from unpaved roads, where it is possible to visually spot surface defects, such as potholes, washboardings, and rutting. Different DCNN models were trained and assessed for the detection of defects on the road surface. In addition, a postprocessing method was proposed to enhance the detection results. The system was developed using the MATLAB platform with several toolboxes, including Computer Vision, Image Processing, Deep Learning, and Parallel Computing. A schematic workflow of the proposed research is shown in Figure 1.

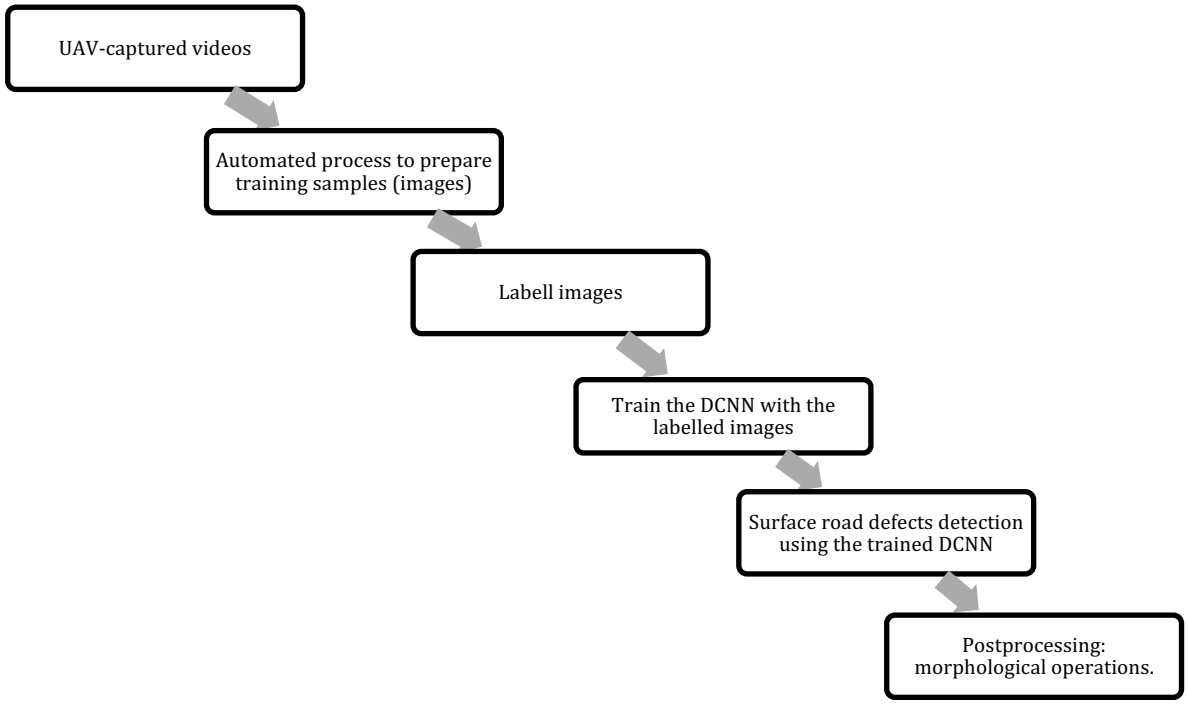

Figure 1: Schematic workflow of the proposed method

1.4 Thesis organization

This thesis consists of five chapters. Chapter 1 introduces the research background and basic concepts in this research area. Further, the research motivations, objectives, and the methodology of this research are presented. Chapter 2 provides a comprehensive literature review on the topics related to this research. Chapter 3 breaks down the framework of the methodology and describes the development of the proposed system. In addition, Chapter 3 explains the tools, software product, processes, and algorithms used to develop and enhance the proposed system.

Chapter 4 presents the results on the tests performed on sets of distinct samples (images), as well as the findings from the postprocessing technique applied to enhance the results, and discussion about the results obtained and potential reasons, and/or solutions for the presented outcome. Chapter 5 presents the conclusions for this research which summarizes the results, discusses the existing limitations, and provides recommendations for future developments.

Chapter 2: Literature Review

2.1 Unpaved roads fundamentals and maintenance

Unpaved roads have a significant role in transportation and service activities in Canada. According to the Transport Canada, unpaved roads account for 60% of the total length of public road networks in Canada (Transport Canada 2018). These roads are critical for the accessibility of remote areas, such as Indigenous communities, local agricultural, mining, and recreational areas. Some of these roads connect farms to the closest cities, making them high traffic roads in seasonal times. Despite the lower construction costs compared to the paved roads, unpaved roads could suffer from frequent damages due to the environmental conditions and traffic load, requiring constant attention, including assessment and maintenance operations (Archondo-Callao 2004). Unpaved roads as referred to in this research are those roads with a surface made of earth material, gravel, or treated gravel, and they are periodically resurfaced with a motor grader (Huntington and Ksaibati 2009).

According to the Government of Canada, provincial/territorial jurisdictions are responsible for the management and maintenance of their highway and road networks (Transport Canada 2021). Condition assessment is a main requirement for effective maintenance of the road networks as it facilitates informed decision making about allocation of limited available resources for maintenance and rehabilitation of the existing roads (Cambridge Systematics, Inc. and Meyer 2007). Conventional road evaluation methods consist of field observation by qualified professionals and extensive fieldwork. These types of assessment could face safety issues, especially on roads with a high volume of traffic. They also require significant time and are labour-intensive (Zhang and Elaksher 2012).

The surface condition in unpaved roads, and the frequency and quality of the applied maintenance program could affect vehicle operation costs by more than 50%, and they also substantially affect the ride quality levels (Archondo-Callao 2004). These findings highlight the importance of the condition assessment in keeping such infrastructure in an acceptable serviceability level.

In order to comprehend the condition assessment process in unpaved roads, it is necessary to describe a typical unpaved road structure, since it has a significant role in the road's performance. A gravel road is composed of a crowned driving surface, shoulder areas, and ditches on the sides of the road as shown in the cross-section illustrated in Figure 2.

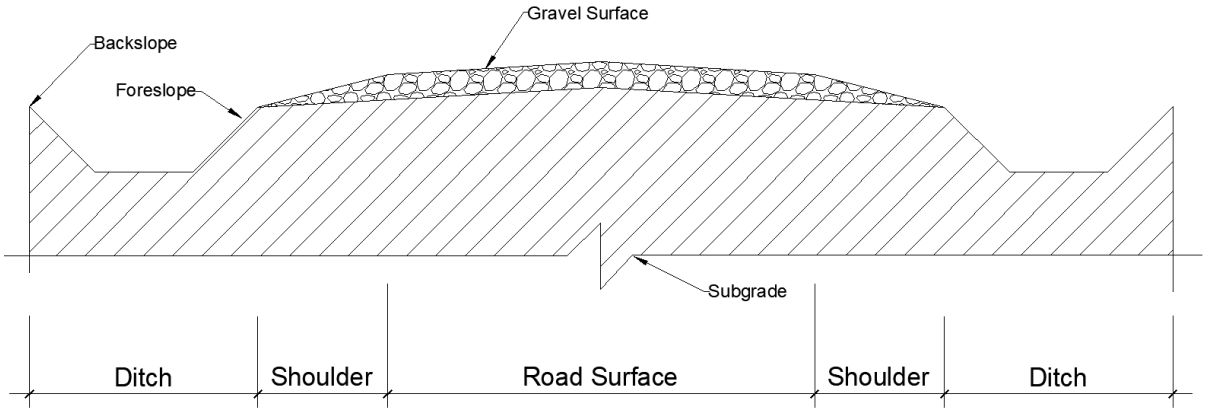

Figure 2: The components of an unpaved road cross-section

The cross-section shape plays an essential role in the road performance, including its maintenance, because this cross-section should keep the water drained away from the road surface. It is known that standing water on the road surface is one of the primary reasons for the distresses and failure of a gravel road (Maine Department of Environmental Protection 2016). According to Zhang (Zhang 2010), rainfalls remove small particles from the crowned driving surface which cause a loss of material and disturb the surface layer gradation. In addition, the water trapped on the road surface can be one of the causes of potholes.

A primordial reason to build a crown into the roadway is to drain water off the roadway quickly. According to MDEP (Maine Department of Environmental Protection 2016), a road crown could be smoothing or super-elevating of the gravel road. The crown can also be defined as building a high point that runs lengthwise along the center of the road so that either side of this high point is sloped gently away from the center toward the outer edges of the road, as presented in Figure 3.

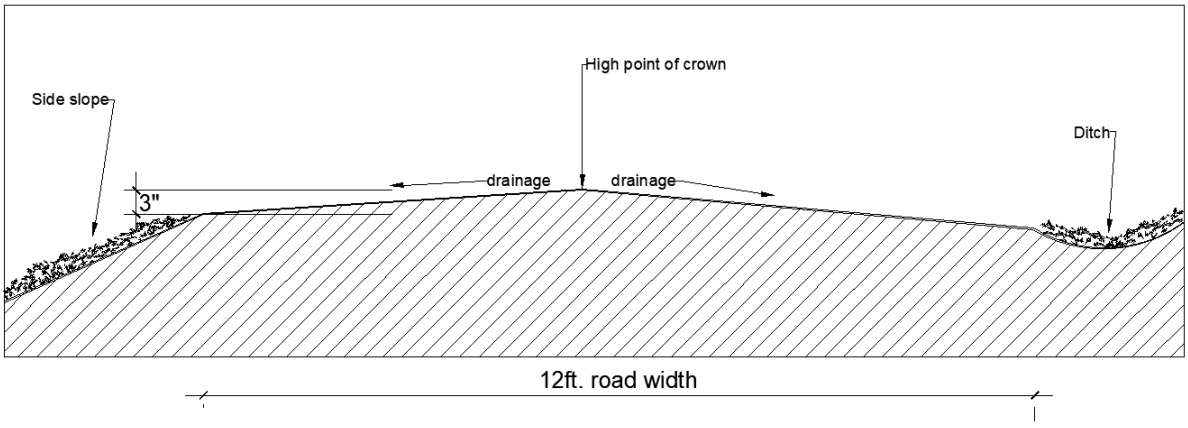

Figure 3: Crown profile: ½ " of crown per foot of road width (e.g., ½ " x ½ x 12' road = 3" crown)

Usually, a gravel road should have a 1/2 inch or 3/4-inch slope per foot of the road width. The MDEP (Maine Department of Environmental Protection 2016) recommends that the crown maintenance must be done annually, because the weather wear and traffic load could deteriorate this mild slop.

Another approach is the super-elevation concept, which similar to the crown, prevents the water from puddling on the road surface. In the super-elevation approach, instead of building a higher point in the center of the road cross-section, it tilts the entire roadway surface (except the uphill shoulder) in one direction. Unlike the crown, a super-elevation will not only drain the water, but it is also built on the horizontal curves as a safety measure, as shown in Figure 4.

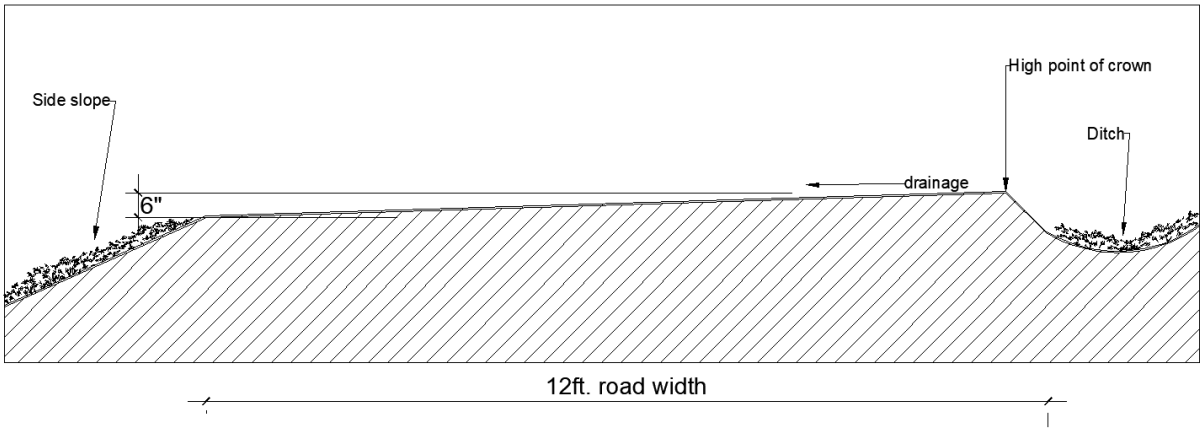

Figure 4: Super-elevation profile: ½ " of super-elevation per foot of road width (e.g., ½ " x 12' road = 6" crown)

The MDEP (Maine Department of Environmental Protection 2016) defines the shoulder area as the region between the roadway edge and top of the ditch. Its width ranges from 18" to 48". The shoulder's main functions include:

- transfer the surface drained water to the ditch.
- fit a snowbank area.
- provide a safe visibility zone and emergency parking space.
- provide structural support for the roadway surface.
- serve as a safety transition zone between the roadway and the top of the ditch.

On the unpaved roads, the shoulders usually have a gravel or grass surface. It is necessary to stabilize the shoulder with vegetation or rocks to avoid erosion. The MDEP (Maine Department of Environmental Protection 2016) recommends that the minimum drop should be 1.5” to 2” for a 2-foot shoulder. For a 4-foot shoulder, the minimum drop should be 3” to 4”. The transitions between the roadway and the shoulder should be smooth for the driver; therefore,

the shoulder should be shaped from the roadway edge, ensuring a seamless transition. The shoulder maintenance is performed by removing winter sands and debris, ensuring the grade is adequate, and the vegetation should be mowed during the Spring and Summer seasons.

In some ideal cases, the road can be built without a ditch. When the local topography favours that condition, the water flows out of the shoulders as a non-erosive dispersed flow of water in a thin layer over the surface. Nonetheless, it is not a usual situation, because the local topography often does not allow this type of design and the road requires a ditch. A ditch is a U-shaped excavation channel adjacent to the road. Its main function is to collect and carry the drained water downward the slope. Some factors must be considered in construction of a ditch, such as the watershed size, degree of the road slope, width of the right-of-way, ditch size and shape, and the soil type.

The ditch maintenance process consists of keeping it clear of obstructions and erosions. It is done by cleaning out the leaves, especially in the Fall, and by stabilizing the ditch with grass, erosion control blankets, or stones. Another measure is to install turnouts in the ditch to reduce the amount of water that flows down in the ditch.

Unpaved roads frequently present distresses and failures due to their structural design combined with environmental and operational conditions, such as weather and heavy traffic. A weak subgrade combined with heavy traffic loads, for example, results in the surface failure, even if its cross-section is shaped according to the standards.

To develop an efficient maintenance plan and keep the roads in an acceptable serviceability level, the operators first need a condition inventory that locates road sections with major distresses, such as rutting, potholes, and washboardings. A conventional road assessment generally consists of visual inspection conducted by a trained expert. Since this type of assessment relies on visual evaluations, the process is time-consuming and labour-intensive,

and could be error prone. Therefore, several studies proposed methods to automate road assessment processes using advanced sensing technologies, such as computer vision and Unmanned Aerial Vehicles (UAV) systems coupled with machine learning (Wu et al. 2019, Dobson et al. 2013, Zhang and Elaksher 2012, Sattar et al. 2018 and Koch et al. 2015).

2.2 Visual methods to evaluate road surface condition

Various road condition assessment methods have been developed for the asphalt and concrete roads over the last decade; however, the same level of efforts have not been applied for the assessment of unpaved roads, namely regarding the application of new sensing technologies. Therefore, it is still common to use traditional methods to evaluate unpaved road networks, which are discussed in this section.

In order to rate the condition of an unpaved road, researchers such as (Walker 1991), pointed out two considerations: First consideration is to assess the drainage, crown condition, and the adequacy of the gravel thickness. Second, the assessment should measure the road surface defects, such as washboardings, ruts, potholes, and dust.

A major study, indicated in (Walker 1991) and conducted by the Transportation Information Center at the University of Wisconsin in Madison, developed a model (called Gravel-PASER system) that introduced a set of criteria for rating unpaved roads. Besides the gravel roads, this system also included criteria for the assessment of asphalt and concrete roads.

The Gravel-PASER manual introduces a visual assessment system that determines a rating scale based on the type and severity of defects, focusing on the type of maintenance that would be more appropriate for the existing defects (Walker 1991). This assessment relies on the judgement of the person responsible for conducting the assessment. This rating system will provide better results when the judgement is made in the field. If the staff cannot conclude by

visual inspection, additional evaluation methods, such as sampling tests, can be used. Although it requires a good knowledge of the road defects, and the responsible staff require extensive background. The candidates can quickly receive training on this rating system.

Walker (Walker 1991) introduced a simplified rating system to document the condition of the gravel roads. This system includes three steps: The whole roadway is parcelled out and categorized according to its pavement thickness and traffic volume. Later an inventory of each parcel is proposed according to its characteristics, such as geometry, traffic volume, and functional classification. Finally, the road condition is determined by assorting the type of distresses, their extent, and severity.

The process of rating a gravel road differs from the rating of the paved roads. By definition, the rating process focuses on determining the type of maintenance each road section will require. To rate a gravel road, the staff should consider three major factors, including two primary factors: the road crown and drainage, and lastly: the adequacy of the gravel layer.

The primary factors, including roadway crown and drainage, can be visually inspected. The third factor, the adequacy of the gravel, needs more information, such as the road thickness and the aggregate quality. A good indicator of the adequacy of the gravel is the existence of distresses on the road surface. These distresses can be manifested as rutting or potholes, which indicate that the road's capacity of carrying traffic loads has been compromised. Afterwards, other distress types, such as washboarding, loose rocks, and dust, will be evaluated (Walker 1991). Walker (Walker 1991) stated that although relevant, such defects usually indicate traffic-related issues and are less critical for maintenance planning.

As discussed above, the road crown is necessary to drain the water away from the road surface. A proper crown maintenance should provide a crown grade between 1/2 and 3/4 inches per ft of road width. To provide an adequate water flow and to avoid the water to flow over the road

surface, drainage is the next primary factor to be inspected where the dimensions of the ditch and the obstructions (e.g., tree branches and leaves) should be assessed. It is also necessary to observe any erosions and to fix or prevent them.

Adequacy of the gravel layer is the third evaluation factor as it plays a major role in the road performance. The gravel layer must provide a smooth driving experience. The process of evaluating the gravel layer mainly includes identifying, classifying, and rating the signs of distress. Surface distresses can be classified into five main groups:

- Washboarding
- Potholes
- Rutting
- Dust
- Loose aggregate

2.2.1 Washboarding

Washboarding, also known as corrugation, is as series of spaced ridges and valleys that are perpendicular to the longitudinal axis of the road and usually have rather similar intervals (Eaton et al. 1989), as presented in Figure 5. It was mentioned that washboarding can be caused by traffic load action and loose aggregates (Eaton et al. 1989; Walker 1991).

Figure 5: Washboarding (corrugation) of an unpaved road surface

In addition to the heavy traffic loads, the MDEP (Maine Department of Environmental Protection 2016) identifies poor road surface material as a cause of washboarding. It states that the lack of fine material (silts and clays) can cause this type of distress. In order to rate washboarding distresses, a guideline classified washboardings according to their severity, dividing them into three severity levels: L, M, and H (Eaton et al. 1989).

The severity level L (low) means that the corrugation (washboarding) depth is less than one inch, and the severity level M (Medium) indicates depths ranging from one to three inches. Finally, the corrugations deeper than three inches are classified as H (High) (Eaton et al. 1989). This classification is based on the PAVER PMS Method, which was developed by the U.S. Army Corps of Engineers and the American Public Work Association. It is possible to classify this type of distress using the concept of Deduct-value, which is presented in Figure 6.

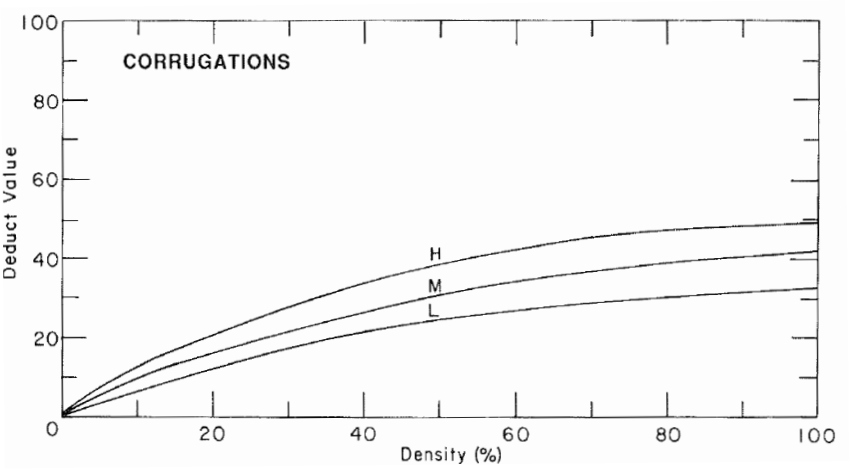

Figure 6: Deduct-value curves for corrugations (Eaton et al. 1989)

Deduct-value is a rating metric proposed in PAVER PMS, based on a number from 0 to 100, where 0 means that the distress has no impact on the road surface condition (i.e., there is no distresses on the road surface) and 100 indicates a very severe impact to the road (failure) which is caused by the existing distresses.

2.2.2 Potholes

Potholes are localized depressions on the road surface. They typically have a diameter less than 3 ft, as shown in Figure 7. The MDEP (Maine Department of Environmental Protection 2016) identifies poor drainage of the road surface and insufficient road crown as the main causes of potholes on the road surface. Eaton (Eaton et al. 1989) stated that the potholes occur when traffic abrades small pieces of the road, and they grow as the water gets trapped inside them.

Figure 7: Potholes on an unpaved road surface

Potholes' extension and depth indicate lack of strength on the road surface and highlight the need for a major repair (Walker 1991). For example, it is a major concern when potholes are more than 4 inches deep and cover more than 25 percent of the road surface area (Walker 1991). Trapped water in the pothole can also accelerate deterioration of the road surface. Accordingly, potholes can be classified into Low (L), Medium (M), and High (H) severity levels using Table 1 (Eaton et al. 1989). In addition, based on the PAVER PMS method, deduct values can be calculated for the potholes similar to the graphical approach presented in Figure 6.

Table 1: Pothole's severity levels according to Eaton (Eaton et al. 1989)

Maximum depth (in)	Avarage Diameter (ft)			
	< 1	1-2	2-3	>3
1/2 -2	L	L	M	M
2 - 4	L	M	H	H
4 +	M	H	H	H

2.2.3 Rutting

Rutting are long depressions that occur on the road surface parallel to the road's longitudinal axis (in the wheel path) (Eaton et al. 1989), as shown in Figure 8. Rutting can be an indicator of heavy traffic volume in the area (Eaton et al. 1989). According to Walker (Walker 1991), a rutting deeper than 3 inches can indicate a lack of sufficient gravel thickness. The MDEP (Maine Department of Environmental Protection 2016) goes further in explaining the possible reasons for rutting in the unpaved roads. Besides the high volume of traffic, ruts also expose a poor road base material, which prevents an efficient drainage, and insufficient ditching can also be pointed as one reason for rutting. All the cited reasons contribute to the softening of the road surfaces, and their combination with high traffic volume cause the rutting.

Figure 8: Rutting on an unpaved road surface

Eaton (Eaton et al. 1989) defined a method for rating of the rutting distresses, which were categorized into three severity levels and integrated into the PAVER PMS Method. The ruts with less than 1 inch depth are classified into the L category. When the rut depth is between 1 and 3 inches, it fits into the class M category and the ruts deeper than 3 inches are categorized

in the H severity level. Then, their deduct values can be calculated similar to the graphical approach presented in Figure 6.

2.2.4 Dust

Dust is a phenomenon that occurs due to the abrasive action of traffic on the unpaved road surfaces, as shown in Figure 9. Several conditions implicate in the dust defect, including gradation of the aggregate layer, traffic volume, and weather conditions. According to Walker (Walker 1991), dust can be a precedent to other severe defects, because it removes fines from the road surface. Dust can also cause safety issues as it can impair the drivers' vision.

Figure 9: Dust on an unpaved road surface (From Oransi 2021)

Eaton (Eaton et al. 1989) classified dust into three severity levels as well. The L severity indicates a thin dust that does not impair the driver's sight. A medium-thick dust cloud makes the traffic slow down because of the low visibility (M), and a thick cloud that obstructs almost the entire sight (H).

Eaton (Eaton et al. 1989) proposed this rating method by driving a vehicle at 25mph and watching the dust cloud. The deducted values for dust are determined as 2 points for low (L), 5 points for medium (M), and 15 points for high (H).

2.2.5 Loose aggregate

Loose aggregate occurs when the road's largest aggregate particles separate from the surface layer, which leads to the loosen base aggregates on the road surface. These loose aggregates can disrupt the traffic flow by collecting the particles between wheels paths. They can also negatively affect the road drainage ability. A sample road with loose aggregate is shown in Figure 10.

Figure 10: Loose aggregate on an unpaved road surface (From Jahren Charles 2015)

In the classification model proposed by Eaton (Eaton et al. 1989), loose aggregate can be classified into three severity levels, similar to the previous distresses. When the depth of aggregate berm is less than 2in, it fits in the severity level “L”. The berms between 2in and 4in are classified as severity level “M”, and they are considered in the “H” level when their berms are larger than 4in.

Unlike Eaton (Eaton et al. 1989), Walker (Walker 1991) proposed a simplified 5-point rating scale based on the Gravel-PASER system, which follows:

- 5 (Excellent): The road's crown is in good condition and its drainage system and gravel layers are adequate. Usually, it occurs on new roads.

- 4 (Good): The road presents good conditions, where its crown, drainage, and gravel layer usually do not need repair.

- 3 (Fair): The road needs small repairs such as grading and, or ditch maintenance.

- 2 (Poor): The road needs major repairs, such as additional aggregate and or major drainage maintenance.

- 1 (Failed): The road should be reconstructed.

The Gravel Road PASER Manual (Walker 2002), as presented in Table 2, follows the evaluation system which was proposed earlier by the same researcher (Walker 1991). This table represents the PASER rating system and corresponding treatment measures.

Table 2: Gravel Road rating system according to the Gravel Road PASER Manual (Walker 2002)

Surface rating	*Visible distress**	*General condition/ treatment measures*
5 Excellent	No distress. Dust controlled. Excellent surface condition and ride.	New construction—or total reconstruction. Excellent drainage. Little or no maintenance needed.
4 Good	Dust under dry conditions. Moderate loose aggregate. Slight washboarding.	Recently regraded. Good crown and drainage throughout. Adequate gravel for traffic. Routine grading and dust control may be needed.
3 Fair	Good crown (3"-6"). Adequate ditches on more than 50% of roadway. Gravel layer mostly adequate but additional aggregate may be needed in some locations to correct washboarding or isolated potholes and ruts. Some culvert cleaning needed. Moderate washboarding (1"-2" deep) over 10%-25% of the area. Moderate dust, partial obstruction of vision. None or slight rutting (less than 1" deep). An occasional small pothole (less than 2" deep). Some loose aggregate (2" deep).	Shows traffic effects. Regrading (reworking) necessary to maintain. Needs some ditch improvement and culvert maintenance. Some areas may need additional gravel.
2 Poor	Little or no roadway crown (less than 3"). Adequate ditches on less than 50% of roadway. Portions of the ditches may be filled, over-grown and/or show erosion. Some areas (25%) with little or no aggre-gate. Culverts partially full of debris. Moderate to severe washboard-ing (over 3" deep) over 25% of area. Moderate rutting (1"-3"), over 10%-25% of area. Moderate potholes (2"-4") over 10%-25% of area. Severe loose aggregate (over 4").	Travel at slow speeds (less than 25 mph) is required. Needs additional new aggregate. Major ditch construction and culvert maintenance also required.
1 Failed	No roadway crown or road is bowl shaped with extensive ponding. Little if any ditching. Filled or damaged culverts. Severe rutting (over 3" deep), over 25% of the area. Severe potholes (over 4" deep), over 25% of area. Many areas (over 25%) with little or no aggregate.	Travel is difficult and road may be closed at times. Needs complete rebuilding and/or new culverts.

** Individual road sections will not have all of the types of distress listed for any particular rating. They may have only one or two types.*

Walker (Walker 1991) estimated that a field rating crew could cover 20 to 40 miles of roadway per day. Thus, a small road network operated by a small township could be covered in a day or two. It might take longer for larger road networks, which highlights the need for automation of these evaluation processes.

2.3 Quantitative measurement of the longitudinal road profile

Several studies used the International Roughness Index (IRI) as a measure to quantify the road surface condition. It is stated that the IRI has been extensively used for assessment of the paved roads, because it is considered a consistent index (Alhasan et al. 2015). The World Bank initiated the IRI development in 1982, seeking to unify the road condition data acquired worldwide and to suit the process for different road profilers (Sayers and Karamihas 1998) .

Road roughness was defined as an inconsistency on the road surface (Archondo-Callao 1999). The IRI is the methodology used to evaluate the roughness of the road surface. It varies from zero to twenty (m/km), being zero referred to as a planar (smooth) roadway, and 20 m/km indicates a road surface that is too damaged (Archondo-Callao 1999). The IRI measures the accumulated vertical movements between the wheel and body of a moving vehicle, divided by the length of the road travelled, thus the results are in the slope units (Sayers et al. 1986).

In addition to the assessment of the road surface condition, IRI could also serve as a tool to measure the overall ride quality and vehicle operating costs (Sayers and Karamihas 1998). A graph was developed to present the IRI ranges matching different road surface conditions, as shown in Figure 11 (Sayers and Karamihas 1998).

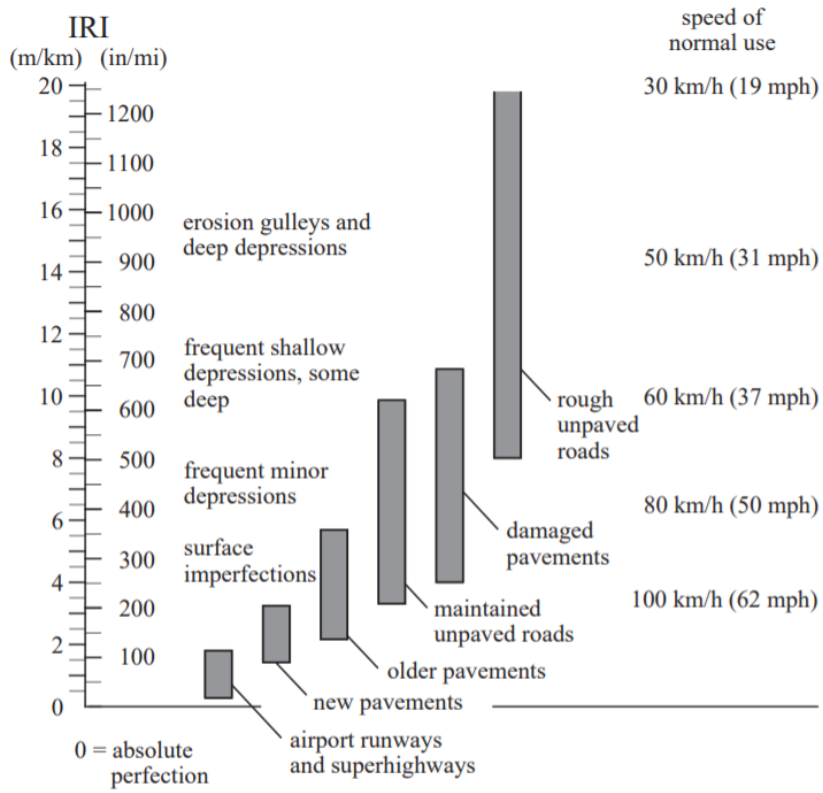

Figure 11: IRI ranges accordingly to the road surface condition (Sayers and Karamihas 1998)

The Guidelines for Conducting and Calibrating Road Roughness Measurements (GCCRRM) advocates four generic roughness measurement methods that fit into many approaches used in the world (Sayers et al. 1986):

- Class 1: Precision profiles
- Class 2: Other profilometric methods
- Class 3: IRI estimates from correlation equations
- Class 4: Subjective ratings and uncalibrated measures

According to the GCCRRM (Sayers et al. 1986), it is necessary to measure a wheel track's longitudinal profile to perform the Class 1 assessment. A range of accurate elevation points closely spaced along the travelled wheel path is necessary to create the IRI basis calculation value. Profilometers can be used to determine the Class 1 method's accuracy, which the GCCRRM stipulates as the most accurate class of measurements (Sayers et al. 1986). The employed profilometer (e.g. Laser profilometer) should be validated against high precision measurement equipment, such as the rod and surveyor’s level, which is considered as the most precise approach to measure the roughness (Sayers et al. 1986).

The GCCRRM established that the distance interval between the surveyed samples should be less than 250mm (4 measures/meter) and the elevation measures' precision must be at least 0.5 mm for the very smooth pavements (Sayers et al. 1986). For rough surfaces, the Precision profiles class can accept measurements with lower precisions.

The rod-level method is the most well-known and accessible profile measurement technique because the required equipment can be easily bought or rented, and the measurement process is straightforward. However, this process is very labor-intensive and expensive. Therefore, the

authors recommended this method when only a limited number of profiles should be measured or the road surface condition is critical, such as airport runways (Sayers et al. 1986).

The Class 2 method includes all the profilometers that can measure the IRI (Sayers et al. 1986). In the Class 2 method, the road profiles are usually measured and computed with high-speed profilometers. The GCCRRM mentioned the APL Trailer as the dynamic profilometer validated by the International Road Roughness Experiment (IRRE) roughness range (Sayers et al. 1986).

IRI can be estimated using correlation equations in the Class 3 method (Sayers et al. 1986), which use measurements acquired through the response-type road roughness measurement systems (RTRRMSs). The RTRRMSs depend on the response measurements provided by sensors installed on a vehicle. The movements of a vehicle allow the measurements to yield roughness properties correlated to the IRI.

The GCCRRM recommends that equations should calibrate the results obtained in the RTRRMSs methods (Sayers et al. 1986). This calibration aims to unify the different results obtained due to the different dynamic proprieties of each vehicle. A method for measuring roughness qualifies as Class 3 if it uses the "calibration by correlation" approach (Sayers et al. 1986).

Class 4 approach includes subjective ratings and uncalibrated measures, which are used when the road assessment does not require a high level of accuracy. The main focus is to obtain a roughness data base (Sayers et al. 1986). This method relies on subjective evaluation, which usually involves a ride to test the road or visual inspections. Alhasan et al. (Alhasan et al. 2015) presented examples that fit the Class 4 method for measuring roughness. However, such assessments did not present any IRI values (Alhasan et al. 2015).

2.4 Computer vision, machine learning, and UAV applications for condition assessment of the roads

Assessing civil infrastructure assets is crucial to ensure that they still meet their service requirements. Such assessments provide the required data to develop models that can predict future conditions and determine if there is a need for maintenance (Koch et al. 2015).

A study by Koch et al. (Koch et al. 2015) brings forward that the infrastructure condition assessments usually rely on a visual inspection performed by qualified professionals (Koch et al. 2015) and highlights that they are susceptible to failures, raising questions about the reliability of manual assessments. As an example of such concern, the study presented the I-35W Highway Bridge collapse in Minneapolis in 2007 due to inadequately conducted inspections.

Automated assessment methods, such automated detection of distresses in the road images, are potential alternative for condition assessment. By using artificial intelligence approaches, including image processing and machine learning, it is possible to automate the infrastructure assessment processes which could reduce the need for human effort and possible errors.

Several research studies demonstrated that the improvements in technology, including digital data capturing and processing, provide vast opportunities to automate data collection and assessment practices (Sahari Moghaddam et al. 2020; Sattar et al. 2018). Namely, there are a growing number of studies that used computer vision algorithms to improve infrastructure condition assessment processes. For example, studies conducted by Wu et al. (Wu et al. 2019) and Cao et al. (Cao et al. 2020) are instances of the combination of infrastructure engineering and computer vision areas.

Koch et al. (Koch et al. 2015) discussed the state-of-art computer vision solutions that were developed to automate the assessments of civil infrastructure assets. Those systems mostly relied on conventional image processing methods (before deep learning), such as template matching, histogram transforms, background subtraction, filtering, region growing, edge and boundary detection, and texture recognition, to detect defects on the surface of different infrastructure assets, such as roads and bridges. In addition to the defect detection, such methods can facilitate classification and rating of the defects, paving the way toward full assessment of civil infrastructure assets (Koch et al. 2015). This study categorized computer vision methods used for detection, classification, and assessment of some defects in infrastructure assets as presented in Figure 12.

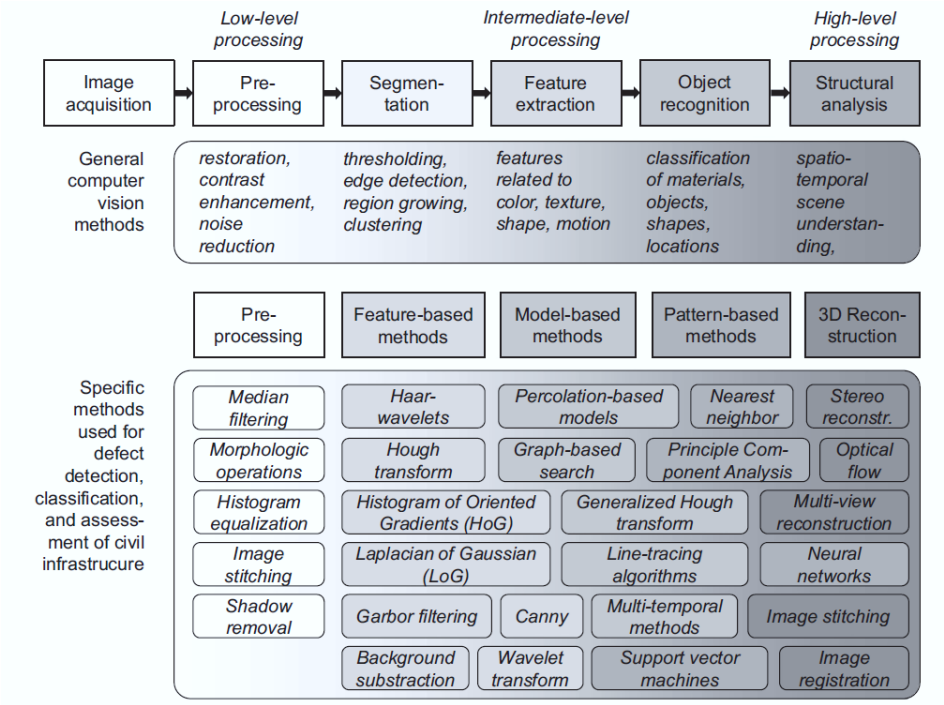

Figure 12: Categorized general and specific computer vision methods for defect detection, classification, and assessment of civil infrastructure (From Koch et al. 2015)

Computer vision techniques are promising tools to improve infrastructure condition assessments. While the defects can be detected by a simple visual inspection, the measurement requires more effort to achieve the accuracy needed for certain types of reports. In some cases,

advanced inspection methods, such as computer vision techniques can provide a better accuracy for the structural assessments (Koch et al. 2015).

There has been a noticeable trend in the research efforts after 2017, as most of the projects have used deep convolutional neural networks (DCNN) for detection of defects. For example, the research presented by Wu et al consisted of collection of a large set of images representing the infrastructure condition, including different types of distresses (Wu et al. 2019). The collected sets of images were used to train DCNN classifiers. Wu et al. (Wu et al. 2019) highlighted that the amount and quality of the collected images are crucial for the DCNN training, being essential to proceed with the next steps. A major issue with the DCNN classifiers is the need for manual labelling of the collected images by trained individuals. The road distresses should be identified and categorized, which in that study, they followed the ASTM D6433-07 standard. They used a smart camera system, including a Raspberry Pi computer, a Pi camera, a Wi-fi adapter transmitter, a receiver, and an AC power cable, to collect images. Later, they programmed the trained DCNN classifier into the smart camera through the Raspberry Pi to streamline the classification process.

Image processing methods and UAV platforms have been also used together to assess unpaved roads. Dobson et al. (Dobson et al. 2013) focused on using an unmanned helicopter to collect images from the roads that were subsequently used for condition assessment of the roads. They used a single-rotor UAV equipped with a Digital Single-lens Reflex (DSLR) camera to obtain images from unpaved road surfaces. It was suggested that the use of UAV and image processing can offer a low-cost alternative for the assessment of unpaved roads. They also pointed out some obstacles that this field of study can face, such as the regulations for operating UAVs. For example, all UAV operators must have a drone pilot certificate to operate a drone between 250 g and 25 kg in Canada (Transport Canada 2019). Dobson et al. (Dobson et al. 2013) used

the structure from motion method to generate 3D scenes of the road surface from the UAV-captured images, which allowed identification of height differences on the unpaved road surfaces as the height difference on the road surface could be a main indicator in most distress types. Using a commercial off the shelf solution, they extracted some information that aligned predetermined size bins. The proposed approach had the following steps (Dobson et al. 2013):

- Used the Bundler software to generate a 3D point-cloud.
- A multi-view stereo algorithm was used to increase the density of the point-cloud. The Patch-based Multi-View Stereo Software was used to perform a finer point-cloud.
- A mask was created by applying a windowed entropy filter to the road surface. This mask represented the road surface, differentiating it from the surrounding areas, such as vegetation. By using a Fourier-based technique, it created a watertight surface from the point-cloud.
- With the use of singular value decomposition, the developed system determined the best plane (z-axis) and then it was rotated to become normal to the road surface.
- By choosing the lower entropy, the road surface was segmented, thus it was possible to analyze the road surface and discarding the adjacent areas.
- Application of the Circular Hough Transform allowed the system to find and calculate pothole's locations and dimensions.
- Gabor filters were used to find ruts and washboarding.
- The Crown was determined by the height-field acquired before.

Another system was developed using an unmanned helicopter equipped with a digital camera to survey unpaved roads (Zhang and Elaksher 2012). This system had an onboard flight control system and a ground control station (GCS) that enhanced the automation level of the imaging process. That system allowed a programmed flight trajectory tracking. An autopilot software controlled the prototype to fly on the desired path and the GCS enabled the digital camera to capture frames automatically. The collected images were used to create a 3D scene of the road which provided a clear view of the surface distresses and enabled a detailed evaluation of the road... A recent project also employed structure from motion method to generate 3D scene of logging roads from UAV-captured images, and then used the 3D scene to estimates the depth of wheel ruts on the roads (Marra et al. 2021).

All these proposed UAV-based systems for assessment of unpaved roads used overlapping images from the surveyed roads to create 3D scenes of the roads and detect distresses (Marra et al. 2021; Dobson et al. 2013; Zhang and Elaksher 2012), but this approach requires multiple overlapping frames from each section of the road which considerably slows the assessment process. Thus, the proposed method in this study aims to accelerate the surveying process by developing a method which requires a single flight pass over a road.

Several studies have investigated methods for automated damage recognition and classification in the asphalt roads. Such studies have developed methods to improve the accuracy of distress recognition and lower the associated costs (Cao et al. 2020). The use of vibration sensor-based to recognize road distresses is another approach for this problem, but the results usually have lower accuracy (Cao et al. 2020; Harikrishnan and Gopi 2017), as the vibration data must be indirectly interpreted. Laser scanning-based systems are another alternative assessment method that can provide a high accuracy (Cao et al. 2020). However, these systems are relatively expensive and have high implementation and maintenance costs (Yamada et al. 2013).

With that summary, image processing techniques (IPTs) have been a promising alternative for defect detection in asphalt roads (Cao et al. 2020). In particular, the dramatic improvement of the image processing methods has had a noticeable impact on the asphalt road assessment in the last few years. But they can still encounter some inaccuracies, mostly due to inadequate background illumination and the asphalt texture itself (Cao et al. 2020). Several studies highlighted machine learning approaches to improve accuracy of the defect recognition on the asphalt roads.

2.5 Deep learning-based methods

The conventional systems proposed in many studies (mostly before 2017) consisted of image acquisition, image processing (including preprocessing and feature extraction), and machine learning (i.e., classification) methods to assess whether the identified regions in images are defects or not. However, there were some issues in these approaches which required improvement, such as lighting conditions, false negatives, and the hand-picked feature extraction of IPTs (Cao et al. 2020). More modern systems, namely in the last five years, have been using end-to-end deep learning methods which do not require separate feature extraction and classification steps, and in addition, the feature extraction processes are automatically carried out.

Figure 13 provides a hierarchical representation of the artificial intelligence field and deep learning concept to help visualize and comprehend it. Deep learning is a sub-class of machine learning which is a sub-field of artificial intelligence. The deep learning approach embraces the concept of the brain's neural structure. The neural network behaves analogously to the human brain, where the Artificial Neural Networks (ANN) would behave similarly to the brain's functions.

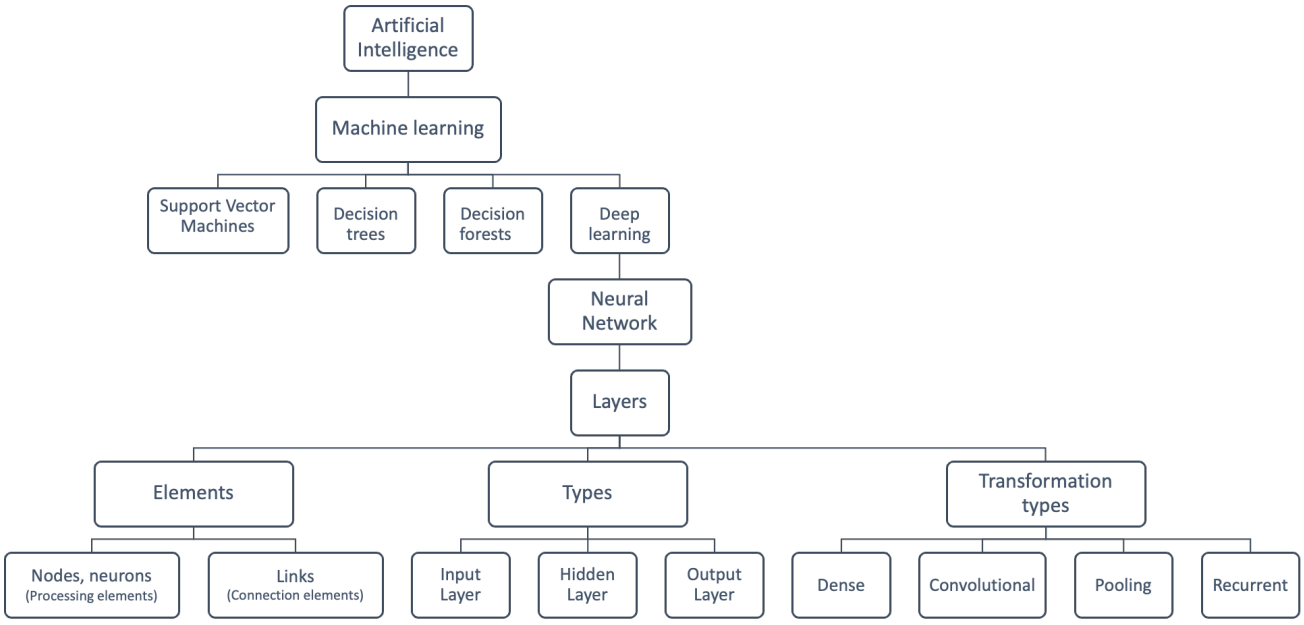

Figure 13: Deep learning hierarchical classification and explanation

A neural network is composed of layers. The neural network layers include processing elements, called nodes, and the connection elements, also known as links. The neural network layers can be divided into the input layer, hidden layer(s), and output layer. The deep neural networks have multiple hidden layers between the input and output layers. An external source is used to feed the input layer, while the hidden layers receive and process the information carried by their prior layers. Finally, the neurons on the output layer process that information to generate the outcome.

The transformations between the input and the output layers are divided into dense, convolutional, pooling, and recurrent layers. Each one of those categories is more appropriate for a specifics process. For example, the convolution is the most used process for image processing purposes (Rawat and Wang 2017).

In the human brain, when the neurons are activated, they produce an electrical impulse. This activation occurs due to multiple stimulations. To develop a similar pattern, the ANNs work

with an activation function, correlating an input value to a specific output. The output of a node is carried by the connecting elements, working as an input for the next node.

It is possible to connect several nodes to one unique node in the following layer, and to include such connections in the network, each link between the nodes should have a weight. This way, the receiving node will receive the weighted sum of the outputs from nodes in the previous layer. Therefore, the optimization of these weights is considered as a major step in the training process of the artificial neural networks.

Given that the purpose of an artificial neural network is to recognize a specific pattern(s) in the input images, this approach requires three steps, including training, validation, and testing. The training step consists of optimizing the weights to obtain the optimal value that would match the correct output classes.

The validation step primarily consists of a procedure similar to the training, creating and comparing predictions on the data and the labels. It differs from the training process only by the weights that are not updated. Finally, a set of images different from the images utilized to train and validate is used for testing the developed network.

As mentioned above, the transformations between the input and the output layers are divided into dense, convolutional, pooling, and recurrent layers. The Convolutional layers are present in Deep Convolutional Neural Networks (DCNN). They operate using filters to detect image patterns, such as edges, shapes, colours, and textures. Simultaneously, the pooling layers simplify the output by performing nonlinear down sampling, which reduce the number of parameters the network would use to learn. Finally, the Rectified linear unit (ReLU) layer provides faster and more effective training, it carries forward to the next layer only the activated features (MATLAB 2021).

The convolution process consists of a filter applied to the regions of the input image, and this filter (kernel) can be represented by a matrix with a specific size, and it slides across the input image until it covers the whole image. The filter performs an operation in each position it passes through, which generates the output (DeepLizard 2019). This process is represented in Figure 14.

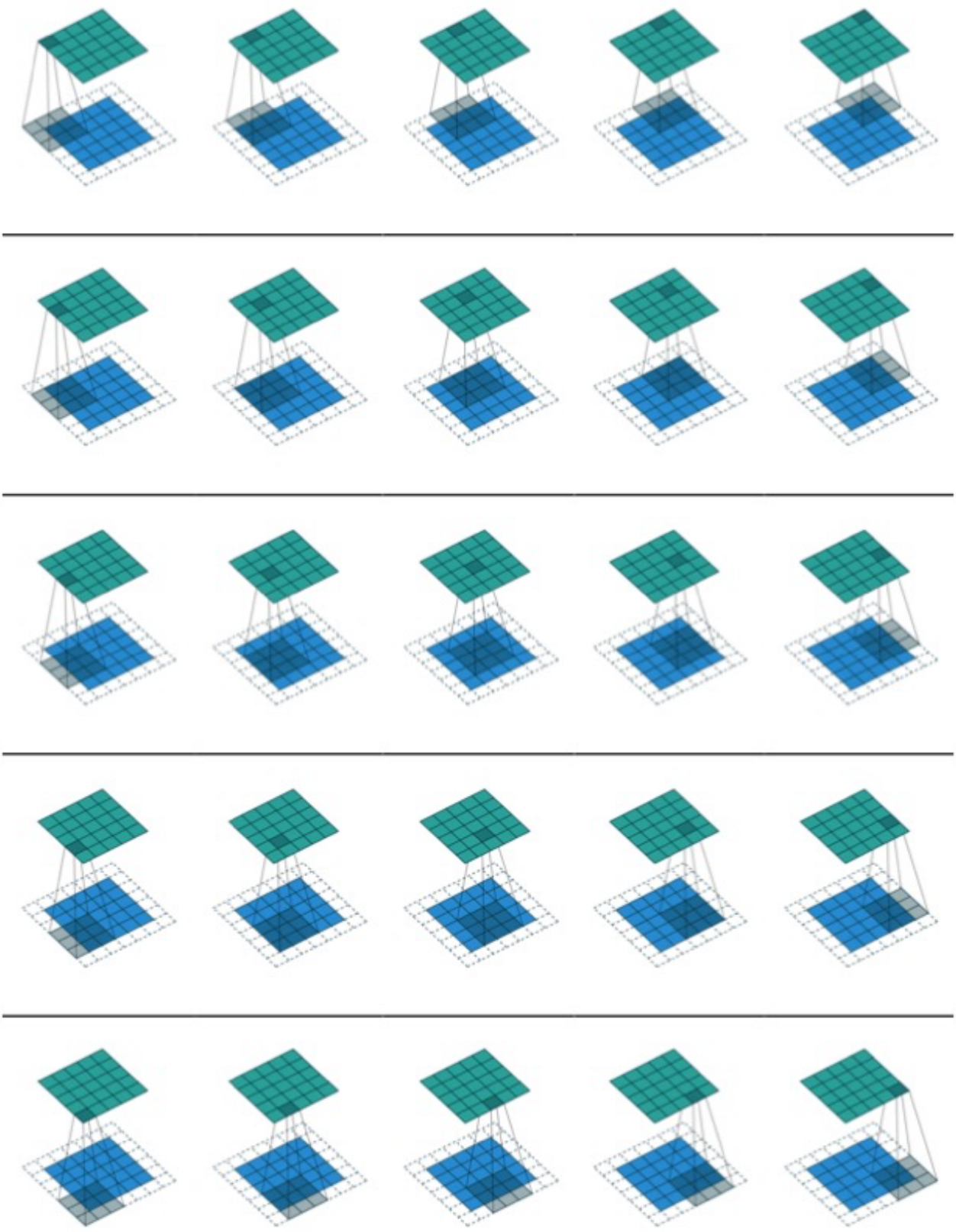

Figure 14: Representation of a convolutional operation (From DeepLizard 2019)

There are different architectures of DCNNs which are used for semantic segmentation and object recognition in images. These networks were pre-trained using a dataset of more than one million images and can classify up to 1000 categories in images. The use of a pre-trained network helps to accelerate the training process on a new image dataset and new classes, and this process is called transfer learning (Mathworks 2019). It has been shown that the transfer learning can accelerate the training process when a pretrained network, which was trained using an unrelated dataset, is used as the base network (Pan and Yang 2009).

The deep learning algorithms extract representative and discriminative features from the bottom to the top level of an input dataset, such as an image (Cao et al. 2020). These extractions are performed automatically and hierarchically, as shown in Figure 15. Several studies showed promising results in infrastructure defect recognition using the deep learning-based methods (Aparna et al. 2019; Butcher et al. 2014; Mandal et al. 2019; Mei and Gül 2020; Song et al. 2018) which used transfer learning on pre-trained feature extraction models such as Inception (Rawat and Wang 2017), Residual network (Resnet) (He et al., 2016), Vgg16 (Simonyan and Zisserman 2014), and MobileNet (Sandler et al. 2018).

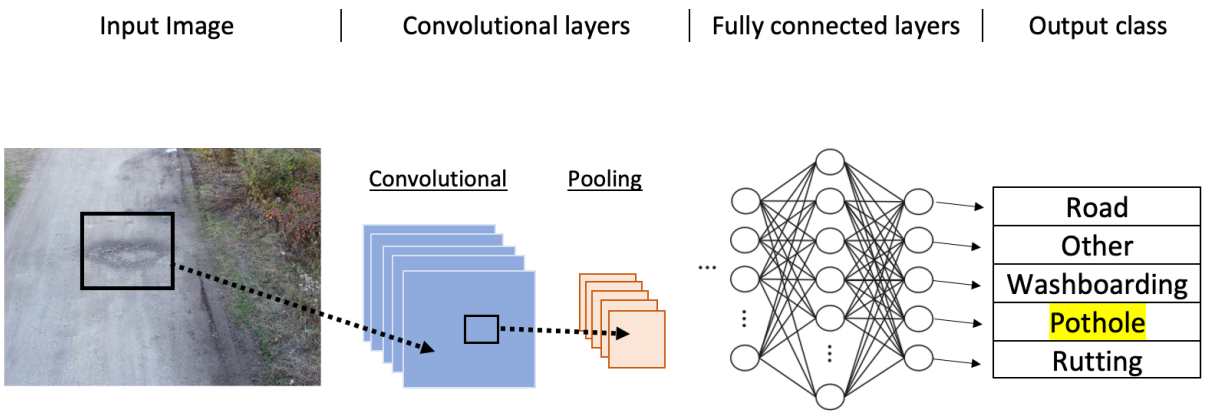

Figure 15: Automatic and hierarchical defect extraction from the bottom to the top level of an inputted data

The Inception model consists of approximating and converting an optimal local sparse structure in a convolutional vision network to readily available dense components. It also works using dimension reductions wherever the computational requirements would increase too much otherwise (Szegedy et al., 2015). In other words, as the network goes deeper, the less computational power it would require.

He et al. (He et al., 2016) explained that the network depth (number of stacked layers) is crucial for the accuracy of the results, questioning how a network depth can affect the results. Further, it was explained that when deeper networks start converging, they face a degradation problem, where the network depth is increased, the accuracy gets saturated and decreases quickly. The Resnet model is brought as an alternative for the degradation problem. It works by fitting the stacked layers to a residual map instead of fitting it to an underlying mapping (He et al., 2016).

The MobileNet architecture aims at a lighter network, and it relies on depth wise separable convolutions to achieve that (Sandler et al. 2018). This model works by factorizing a standard convolution into a depth wise convolution. It applies the regular convolutional operations in the input layer, while it applies the depth wise convolutional operations in the following layers (Howard et al. 2017). The VGG16 model is another popular DCNN architecture. It has a total of 16 layers, including thirteen convolutional layers and three fully connected layers (Simonyan and Zisserman 2014).

Chapter 3: Methodology

This research aims to develop a framework to enhance the automation level of the condition assessment processes in the unpaved roads. It proposes a system composed of UAV-based imaging for data collection and artificial intelligence for distress recognition on the road surfaces. The collected data included UAV-captured videos from unpaved roads, where it is possible to visually spot surface defects, such as potholes, washboardings, and rutting. MATLAB platform with several toolboxes, including Computer Vision, Image Processing, Deep Learning, and Parallel Computing, were used to develop the methods used in the proposed system.

The schematic workflow of the proposed system is illustrated in Figure 16. In this approach, a large number of frames were extracted from the UAV-captured videos and were manually labelled and used for the training of DCNN-based classifiers using the transfer learning approach. In addition, a postprocessing method was proposed to improve the results. Following subsections describe the details of the methods used in this research.

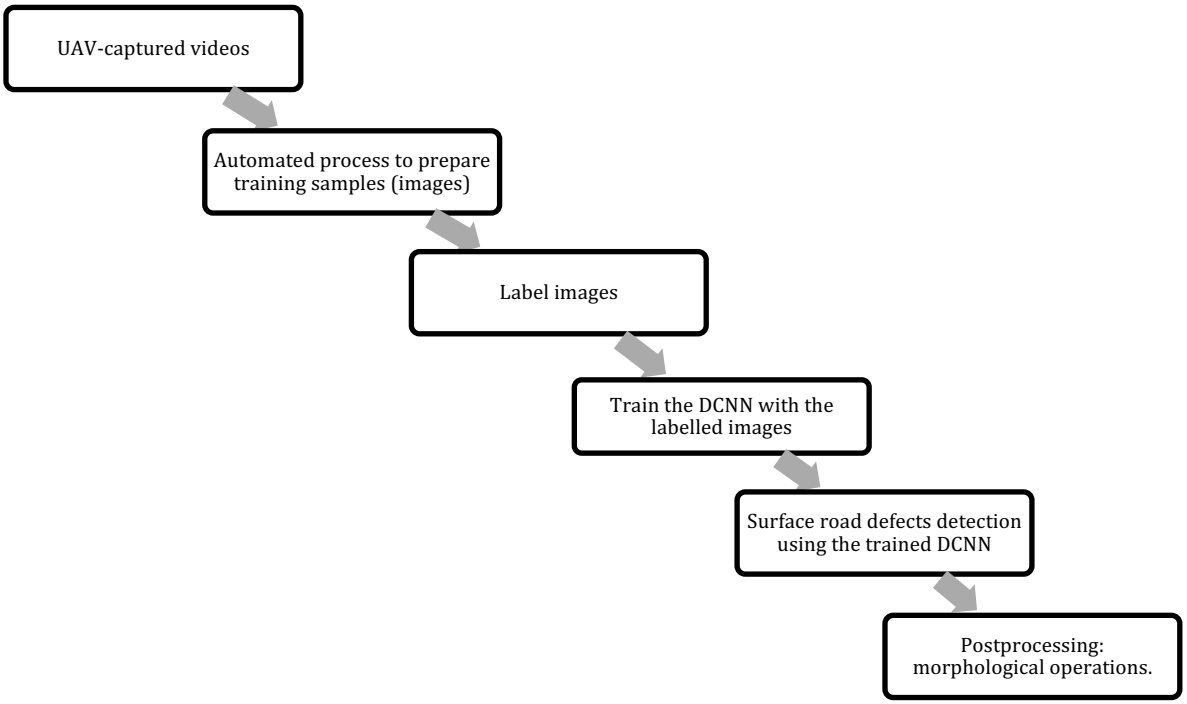

Figure 16: Schematic workflow of the proposed method

3.1 Data acquisition

The videos from the roads were captured using a micro-UAV, named Mavic Mini, which has a takeoff weight of 249g, with folded dimensions of 40×81×57 mm, and unfolded dimensions (with propellers) of 245×289×55 mm. This drone can fly up to 30 minutes with a fully charged battery. It has a built-in camera with 1/2.3" CMOS sensor and 12 MP resolution (Da-Jiang Innovations 2021). The Mavic Mini records videos in the MP4 format with up to 2.7k (2720×1530 pixels) resolution. The photos are captured in the JPEG format in two aspect ratios and sizes, including 4:3 with 4000×3000 pixels and 16:9 with 4000×2250 pixels. Figure 17 shows this UAV that can be controlled by a smartphone through its flight.

Figure 17: Mavic Mini Aircraft

As previously mentioned, the Canadian Aviation Regulations (CARs) stipulate that operation of drones that weigh 250g up to 25kg require a drone pilot certificate (Transport Canada 2020). The Mavic Mini model was chosen in this research to avoid the requirements of the CARs. The Canadian Aviation Regulations also require that a drone should not fly up more than the maximum altitude of 122m. It must fly away from bystanders, at a minimum horizontal distance of 30 metres for basic operations, away from emergency operations and advertised events. It also should avoid forest fires, outdoor concerts, and parades. It must fly 5.6 km away from the airports and 1.9 km away from the heliports and outside controlled airspaces (Transport Canada 2020).

The flight altitude of the UAV was maintained between 5m and 6 m from the road surface and the pitch angle of the UAV was set at -20˚ from the horizontal line during the data collection. The video resolution of 1920 x 1080 pixels was selected and the vertical field of view of the camera was 83˚. If the drone flies at the altitude of 6 m from the road surface, the bottom half of the frame will cover about 13.2 m of the road surface, as shown in Figure 18. Nonetheless, the covered road surface distance can vary based on the geometrical proprieties of the road, e.g., due to the slope of the road and curves (Nasiruddin Khilji et al. 2021). These videos were

captured from more than 10 different unpaved roads within 100 km vicinity of Thunder Bay, Ontario.

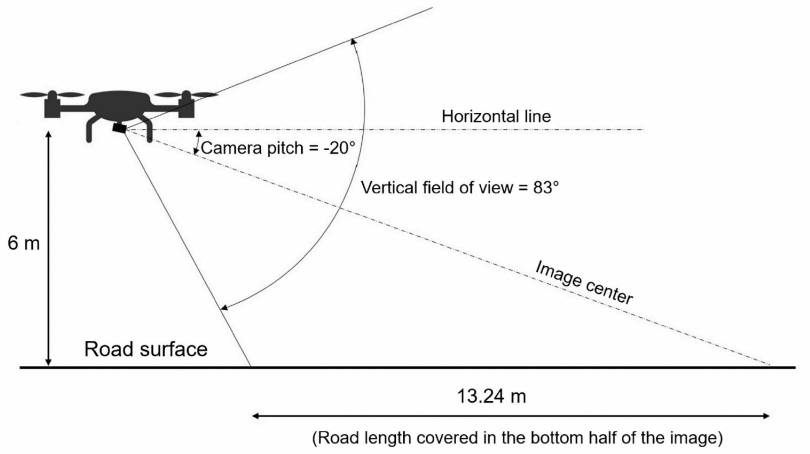

Figure 18: UAV field of view during flight (From Nasiruddin Khilji et al. 2021)

Figure 19 shows a sample frame extracted from the video captured using the proposed setup. A MATLAB code was developed to automate the process of frame extraction. This step is discussed in the next section (3.2).

Figure 19: A sample captured frame

3.2 Data preparation process

An automated process was developed to prepare training samples which includes two steps: The first step grabbed frames from the videos (see Figure 20. a), where it was set to get frames on a certain interval (e.g., every 4 seconds). The second step consisted of cropping extracted images to focus on the road surface by excluding surrounding areas, such as vegetation, and setting those images in a similar size (400x300 pixels) and aspect ratio of 4:3 (see Figure 20. b). That way, the defects become more visible for labelling. The codes utilized for the data preparation process can be found in the Appendix. The results of such a data preparation process can be seen in Figure 20.

(a)

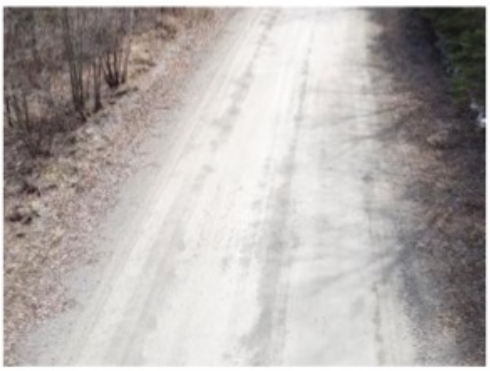

(b)

Figure 20: a) Image frame acquired from a captured video; b) frame cropped and resized

3.3 Image labelling

Since the supervised learning approach is used to train the DCNN classifiers, the training process requires a large number of labelled training samples. The labelling process consisted of manually labelling each prepared frame. All the training images were resized to 400 x 300 pixels. The size of training images might seem small, but this size was determined to create a balance between the massive required computational power and the available computing resources (e.g., GPU, CPU, and RAM). The labelling process was the least automated portion of this research because it required significant amount of human effort to label more than 1000 images. Most of the labelled images were used for training and the rest were used for the testing purpose. This step provided a base for the training process of the DCNN classifiers, as a solid training process is based on the variety of patterns and features available in the training samples, which can consequently enhance the performance of the classifiers. The labelling process was performed using the Image Labeler app available in the Computer Vision toolbox of MATLAB® 2020b software. The images were labelled on a pixel level using the polygon tool in the Image labeller App. Figure 21 depicts the steps taken to label images.

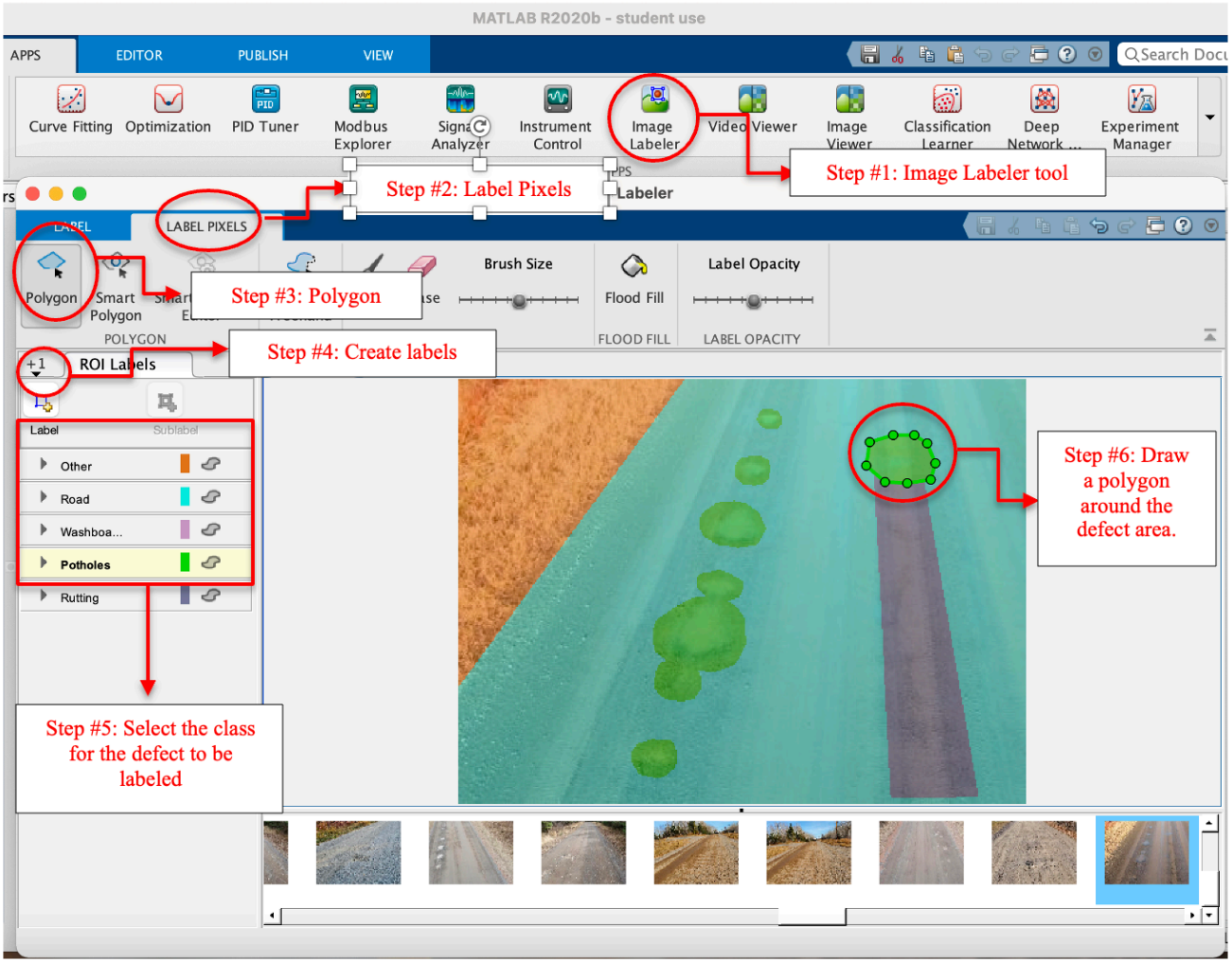

Figure 21: Image labelling process using Image Labeler tool of MATLAB® 2020b software

The labelling process was carried out in three sessions of five hundred and sixty, seven hundred, and one thousand images, to assess the effect of training numbers on the performance of the classifiers. Recent studies showed that the number of images used to train the classifiers can affect the performance of the DCNN (Mei and Gül 2020; Dung and Anh 2019), such studies used 500 images or less to train the classifiers using the transfer learning approach with promising results. Thus, it can be stated that the presented models were trained with enough samples.

The same labelling process was applied in the testing dataset, for this dataset it was labelled one hundred and twenty-two images, as showed in Section 3.5. Figure 22 shows three samples of manually labelled images, in which the labels are overlayed on the original images.

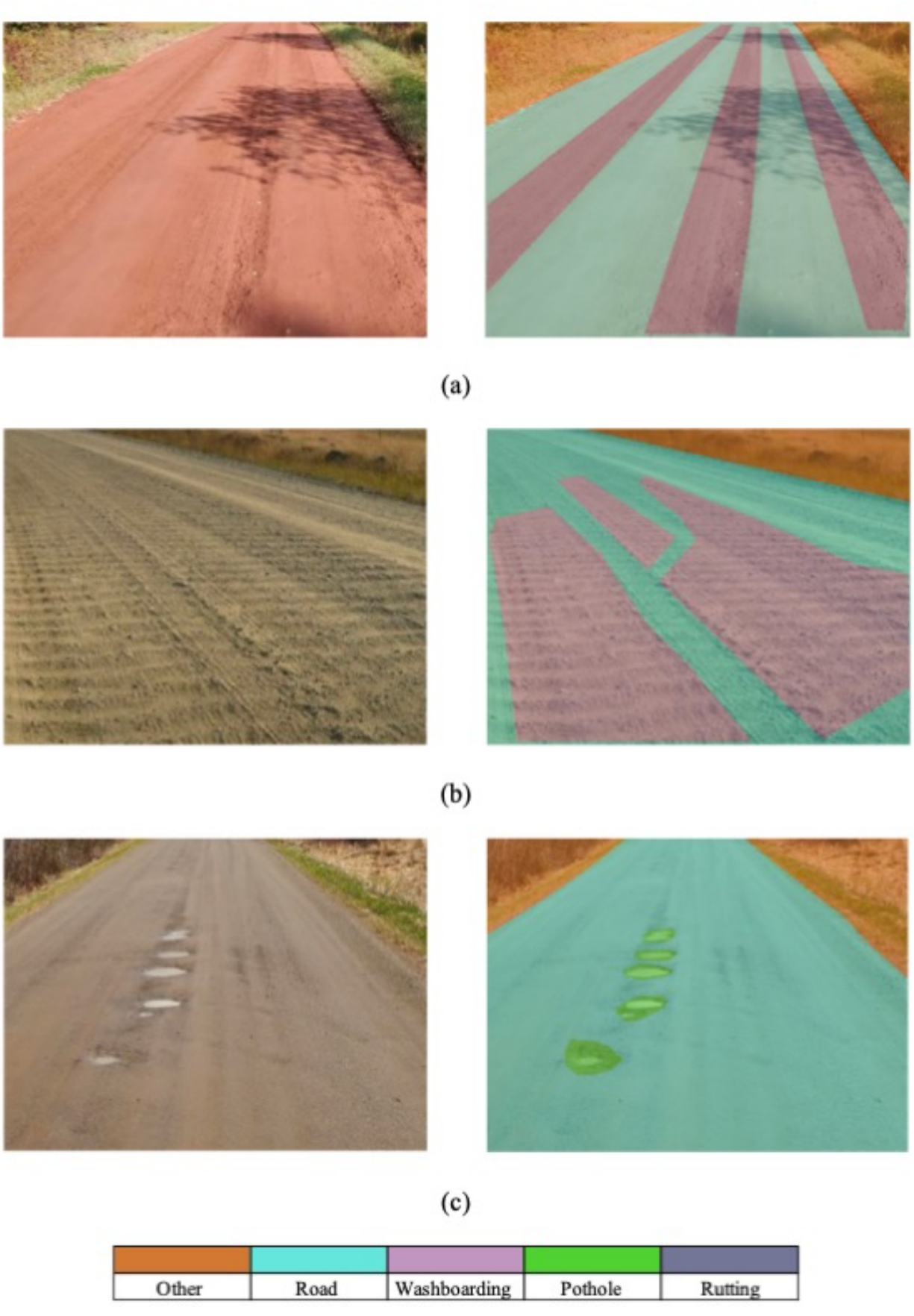

Figure 22: Sample labelled images: a) Rutting; b) Washboarding; c) Pothole

3.4 Training DCNN classifiers

The transfer learning approach was used to train defect classifiers using three pre-trained DCNN architectures, including MobileNetV2, ResNet50, and Vgg16. These architectures are discussed in Chapter 2, and previous research showed a great performance of these three networks architecture in semantic segmentation, specially related to infrastructure's defect detection (He et al. 2016; McLaughlin et al. 2020; Sandler et al. 2018; Simonyan and Zisserman 2014; Yang and Ji 2021).

These three network architectures were previously trained using more than a million images from the ImageNet database (ImageNet 2020) for generic object recognition. The chosen architectures differ based on their proprieties as shown in Table 3.

Table 3: Pretrained DCNN proprieties (Mathworks 2019)

Network	Depth	Size	Parameters (Millions)	Image Input Size
mobilenetv2	53	13 MB	3.5	224-by-224
resnet50	50	96 MB	25.6	224-by-224
vgg16	16	515 MB	138	224-by-224

The training process was performed using the machine learning toolbox of MATLAB® 2020b software. The stochastic gradient descent with the learning rate of 0.01 and the momentum value of 0.9 was employed to carry out the training process. The labeled training images were augmented to enhance the variety of training images by random X and Y translation, and right and left reflection of pixels. The training was done in batches of six images with 100 epochs, when the loss rate was plateaued. The training sessions were performed using GPU-based parallel computing on a desktop computer with the following specifications:

CPU: Intel® Core™ i7 9700 (8-Core, 12MB Cache, up to 4.7GHz); GPU: NVIDIA® GeForce GTX® 1660Ti 6GB GDDR6; RAM:16GB DDR4; and OS: Windows 10.

The training processes took from 2.5 to 4 hours to train each of these models, and the training process was run three times. For each round, extra images were added, the first training process included 560 images, while the second run had 700 images (including 560 images from previous session), and the third had 1000 images (including 700 images from two previous sessions).

3.5 Testing and postprocessing

The trained deep neural network models were developed to assess the surface condition of different unpaved roads. A new set of images was used to perform such an assessment. These images were collected using the same procedures performed to collect the set of training images. This test dataset included one hundred and twenty-two images; a few samples are shown in Figure 23.

Figure 23: Sample of testing images

Each deep neural network model (MobileNetV2, ResNet50 and Vgg16) was trained three times (560, 700 and 1000 images), providing nine different classifiers to test. The testing process was developed in two steps. First, the set of 122 images were manually labelled, using the same process described in section 3.3. However, the test images had varying sizes (e.g., 640 x 480, and 400 x 300 pixels). Then all the trained classifiers processed the test images. Figure 24 provide a sample of manually labelled image and the result of segmentation on the same frame.

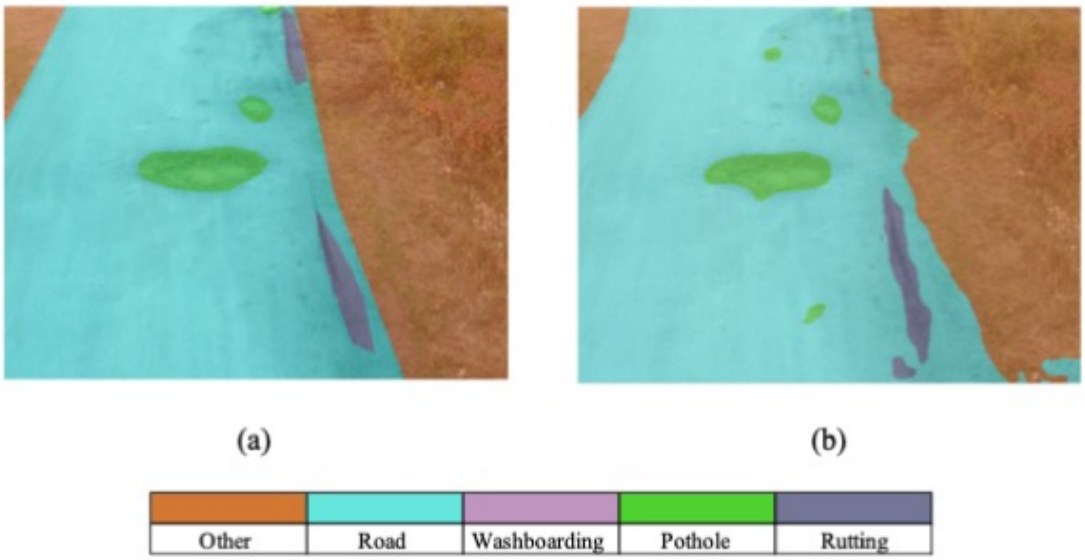

Figure 24: a) Image manually labelled; b) DCNN segmentation using mobilenetv2 trained with 700 images

The results of segmentations were compared against the manually labelled ones, using the Intersection Over Union (IOU) metric, which measures the overlapping between the manually labelled image and the segmentation result by the deep convolutional neural network. The concept of IOU can be seen in Figure 25, where it shows the overlapping areas of the samples presented in Figure 24.

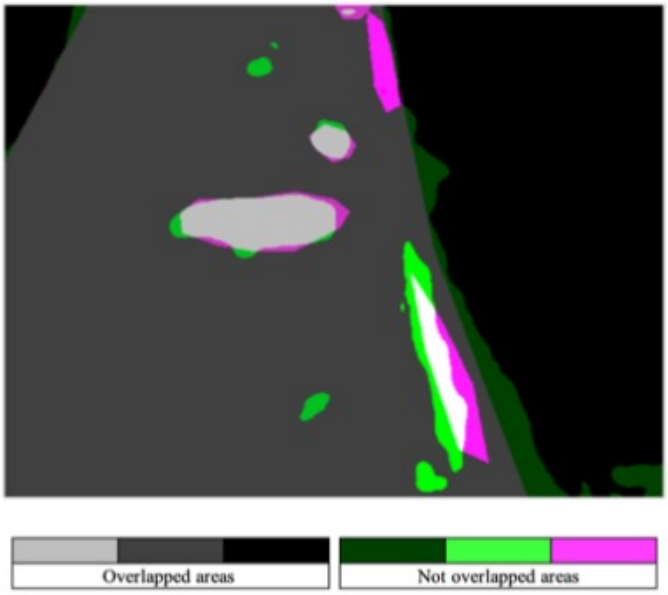

Figure 25: Intersection over union of defect showed previously

The IOU is calculated as: IOU = overlapped area/ (overlapped area + not overlapped areas). As mentioned before, the recent machine learning approaches for image processing methods can still produce errors, including false positives, and the reasons for such errors are discussed later in Section 4.5. Therefore, a postprocessing method was proposed in this research to mitigate such an issue.

The proposed method consists of computing algorithms to binarize the segmentation result of each defect class, and then the morphological opening is applied to remove small, isolated noises and retain the larger elements. Finally, the morphological closing is applied to fill the gaps and connect adjacent elements which might have been segmented as a few separated patches. This study investigates also, if such procedure could either provide more errors or not, considering that when the morphological openings are applied to close and fill small gaps, it can remove small defects instances, such as potholes. The possible outcome of such post-processing is discussed in Section 4.5 of this thesis.

An example of the proposed methodology is shown in Figure 26, in which Figure 26 .b shows the initial segmentation result, and Figure 26 .c shows the binary mask of the pothole class. As it can be seen in Figure 26 .d, many small patches are removed by the morphological opening, and adjacent remaining particles are connected in Figure 26. e. Figure 26. f shows the image with the postprocessed segmentation result.

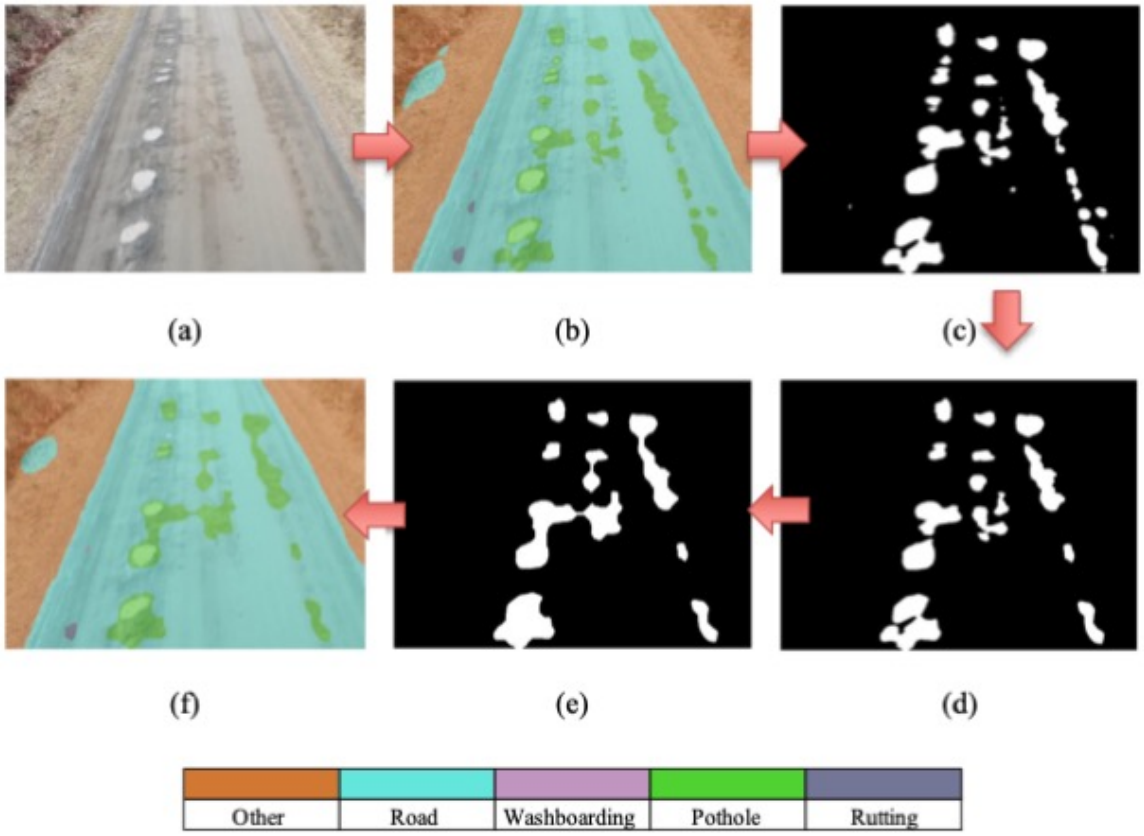

Figure 26: a) raw image; b) overlaid segmented image; c) binary mask of the pothole class; d) mask after morphological opening; e) mask after morphological closing; f) segmentation after postprocessing

The false-positive instances can often be the result of light variations on the image and vegetation shades on the road surface, as shown in Figure 27, where the red arrows indicate false positives.

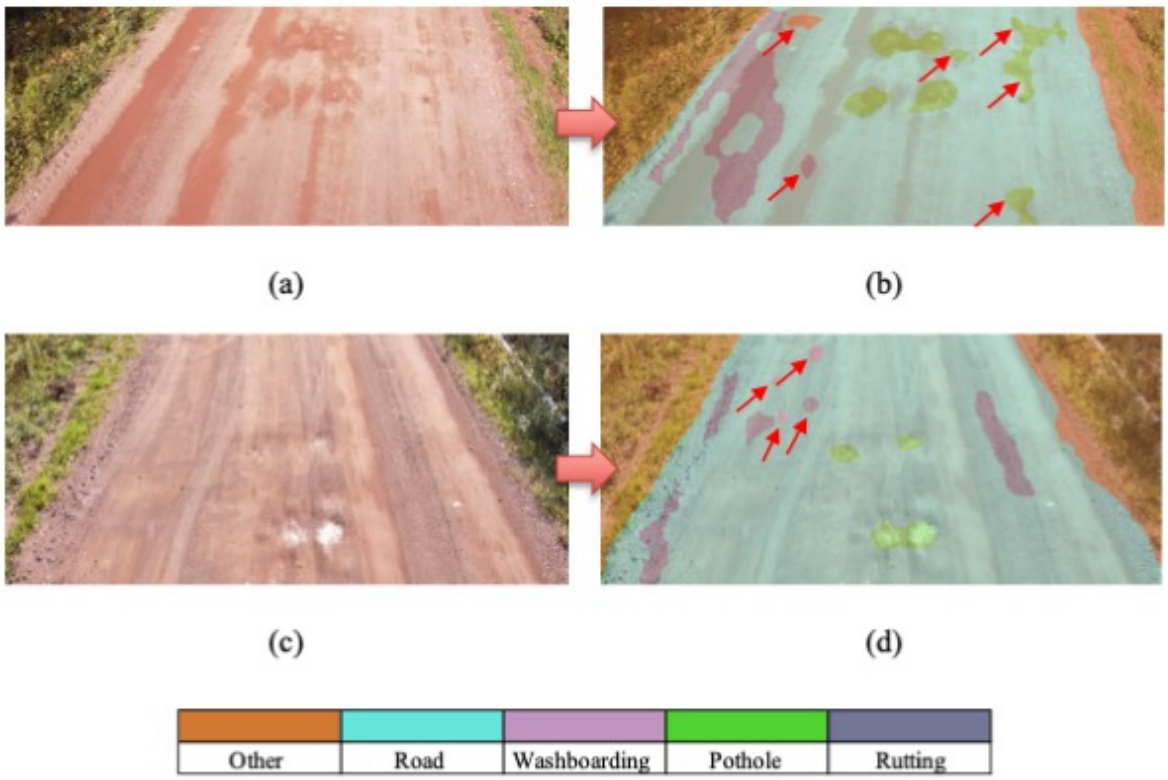

Figure 27: Road surface segmented with DCNN using Mobilenetv2_1000 for the same pothole: a) raw image obtained flying in the same direction of light; b) DCNN segmentation of image "a"; c) raw image obtained flying against the light; d) DCNN segmentation of image "c"

To reduce possible errors and optimize the region of interest in the captured frames, DCNN classifier was used to segment the road surface and limit the region of interest. It was performed by applying a DCNN classifier trained to segment the road surface, making it possible to exclude the surrounding areas, such as vegetation. This method reduces the required computational power than using the entire image. It also decreases the possibility of false positives.

The DCNN classifier used to recognize the road surface is part of the previous research by another graduate student in the research team (Nasiruddin Khilji et al. 2021), compounding a whole study on the automation of unpaved road assessments. In this method, the DCNN classifier segments the pixels into unpaved road and others (Figure 28. b). Then, similar to the previous part, morphological opening and closing were used to unify the binarized road's

segmentation result, which allows excluding surrounding areas and possible noises (Figure 28. c). Then the frame is cropped around the unified road segment (Figure 28. d) and the bottom part of the frames is used for detection of the distresses (Figure 28 e and f). This way, the system will assess the distresses that are closer to the drone, and it excludes assessment of the farther areas which might result in errors. As the drone continues its flight over the road, the upper half of the frame will appear in the bottom half of the subsequent frames and will be processed.

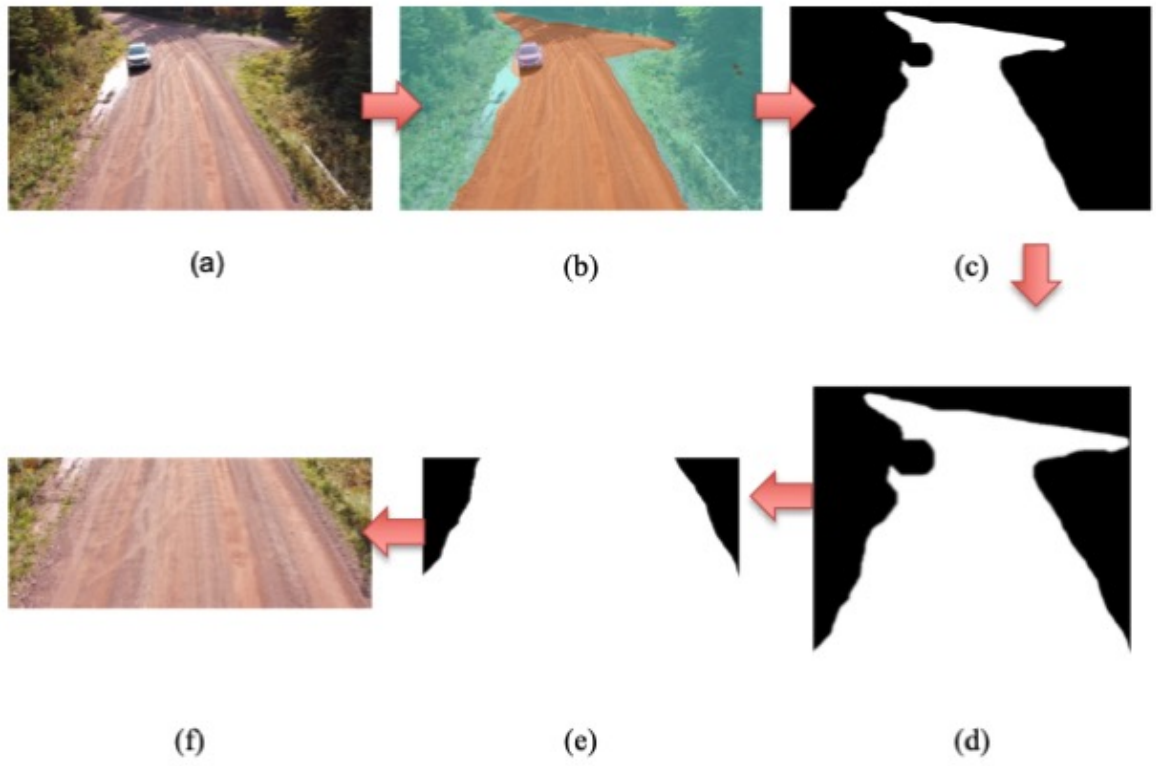

Figure 28: Road segmentation: a) raw image; b) overlaid segmented image; c) binary mask of the road surface; d) trimmed surrounding areas to reduce noise; e) binary cropped bottom half of the road; f) cropped bottom half of the road

As mentioned before, the Intersection Over Union is one of the common metrics to assess the performance of the classifiers in segmentation of the areas of interest. However, a more objective assessment approach is Object Level Detection, which assesses the performance of

the classifiers in detection of individual defect instances, rather than the pixel-level identification. The results can be presented in terms of Accuracy and Precision which are calculated based on the number of true positives, false positives, and false negatives. Accuracy and Precision are calculated using the Equation 1 and Equation 2.

Equation 1: Accuracy	**Equation 2: Precision**
$A = \frac{TP}{(TP + FN)}$	$P = \frac{TP}{(TP + FP)}$
A= Accuracy	P = Precision
TP= True Positives	TP= True Positives
FN = False Negative	FP = False Positive

Figure 29 shows the comparison between manually labelled defects (Figure 29. a), and the defects identified by the DCNN segmentation (Figure 29. b). The red circles in Figure 29. b indicates True Positives (TP) for potholes, the red "X" s represents False Negative (FN) for potholes, and the blue rectangle indicate a True Positive (TP) for rutting. Considering the scenario showed, there are 6 TP and 2 FN for potholes, and 1 TP for rutting. By applying Equation 1 and Equation 2, the accuracy rates of 75% and 100% are calculated for potholes and for rutting, respectively. Precision rate is 100% for both potholes and rutting classes, as no false positive is detected.

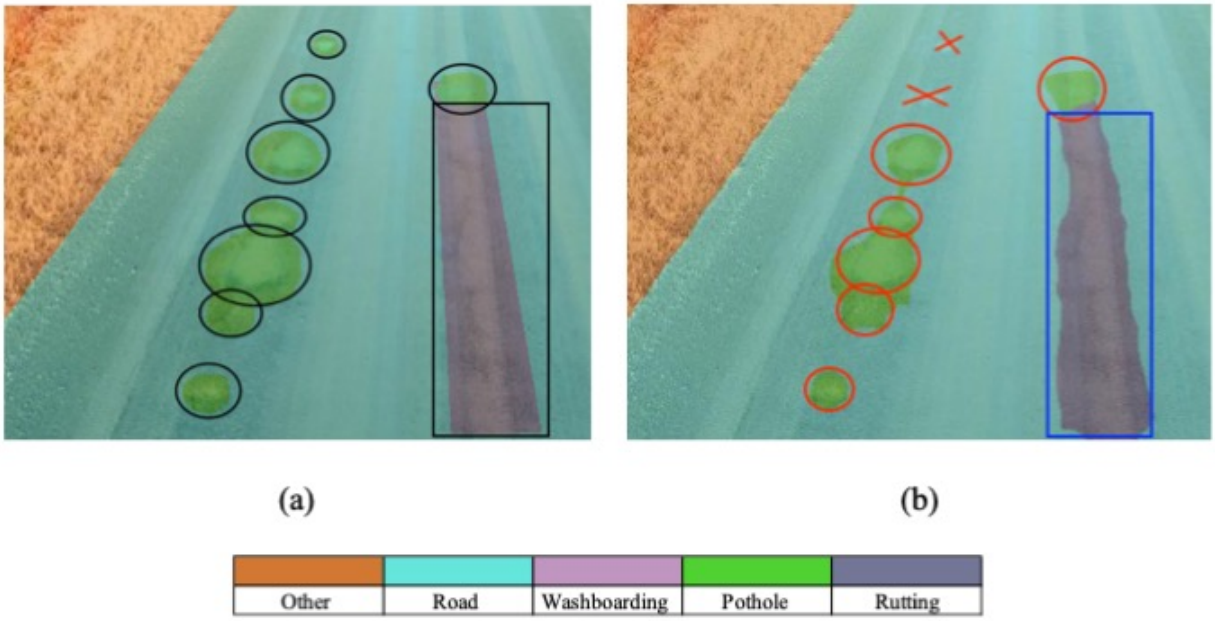

Figure 29: a) manually labelled image; b) DCNN segmentation with the Mobilenetv2 trained with 1000 images

3.6 Defect distribution, case study of potholes

Going further, it is also possible to integrate this method with existing classification methods, such as the PASER rating system (Walker 1991). Therefore, the last part of this research investigates application of the developed image processing and machine learning methods in the PASER system.

The proposed method consists of quantifying the defects distribution over the unpaved road surface. This quantification is proposed by applying the DCNN on an input image (see Figure 30.a), to recognize the road surface, and defects (see Figure 30.b), and then creating a binary mask with the results obtained from the DCNN segmentation (Figure 30.c and .d). For example, black pixels indicate the road surface in Figure 30.c and their population could be counted. Then the mask for the pothole class is created (Figure 30.d) and the number of corresponding pixels is measured. This way, it is possible to determine the defect distribution over the road surface. The developed code for this process can be found in the Appendix.

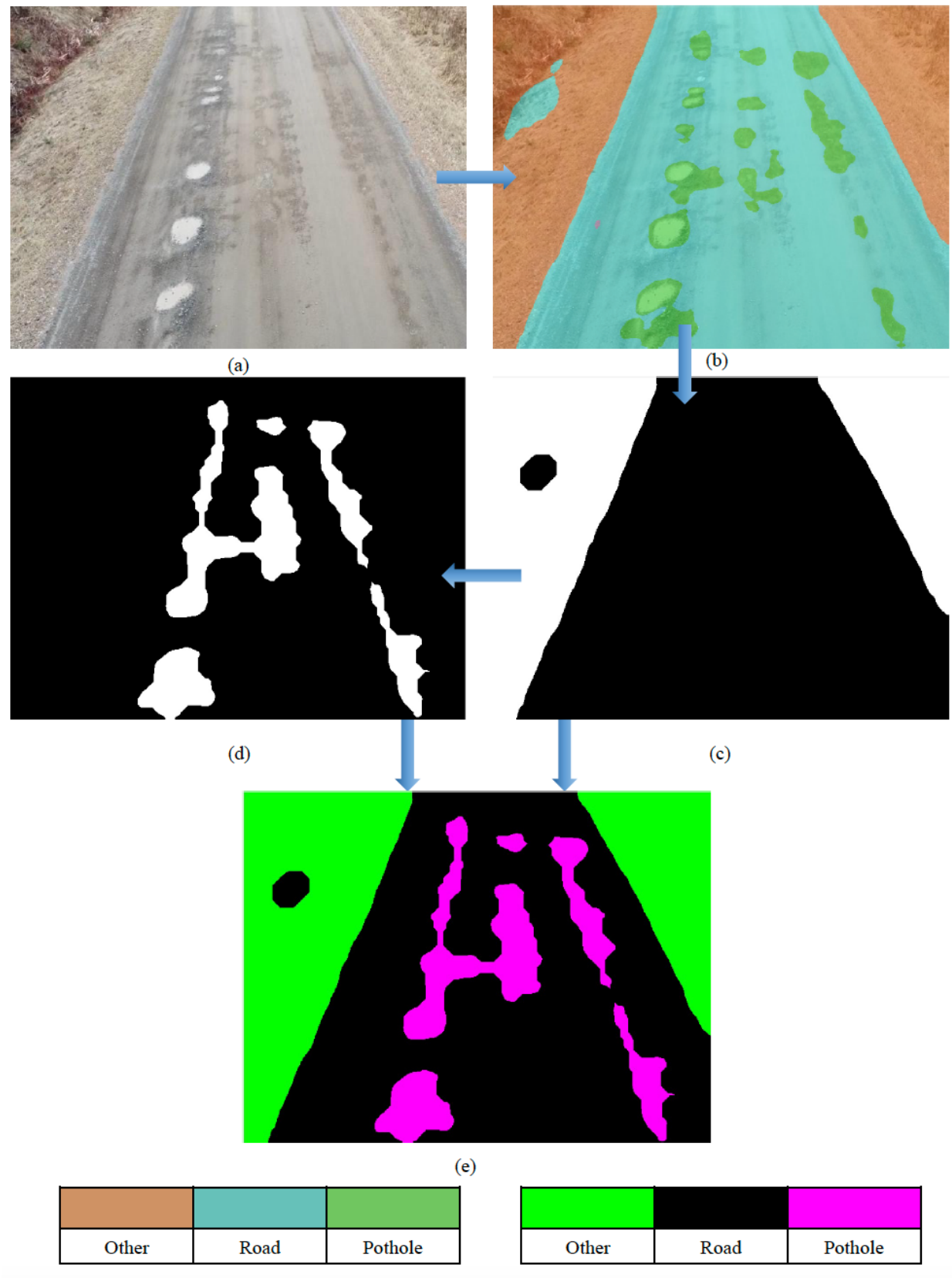

Figure 30: a) Input image; b) DCNN segmentation (Mobilenetv2_1000); c) Surface Road binary image obtained from the DCNN segmentation; d) Pothole binary mask from DCNN segmentation; e) outcome integration

Chapter 4: Results and Discussion

This section presents four distinct test setups and analysis using the trained DCNN distress classifiers, which include assessment of Intersection over union (iou), object level detection, light deflection over the road surface, and defect distribution over the road surface. The last section discusses the findings and challenges encountered in this research study.

4.1 Intersection over union (iou)

As previously discussed, iou is one of the main metrics used to assess the performance of DCNN classifiers in this research, which measures the overlapping of the manually labelled areas with the results of the segmentations by deep convolutional neural networks.

The test dataset included 122 images, and each trained classifier (9 classifiers in total) processed test images twice: Once with the regular code where it only used the DCNN classifier to segment the defects, and the second code where the morphological operations were applied after segmentation to reduce noises, such as small patches and/or false positives. The average of ious on the 122 test images without morphological operations are shown in Table 4 and Figure 31. While the Table 5 and Figure 32 Show the results with morphological operations.

Table 4: Average ious for DCNN distress segmentation without morphological operations

	Without morphological						
classes	Resnet50_560	MobilenetV2_560	Resnet50_700	MobilenetV2_700	vgg16_700	Resnet50_1000	MobilenetV2_1000
Other	86	86	90	86	89	90	89
Road	84	83	88	85	88	87	87
Washboarding	29	30	35	31	30	24	23
Potholes	30	30	34	37	31	32	35
Rutting	6	8	17	12	15	18	19

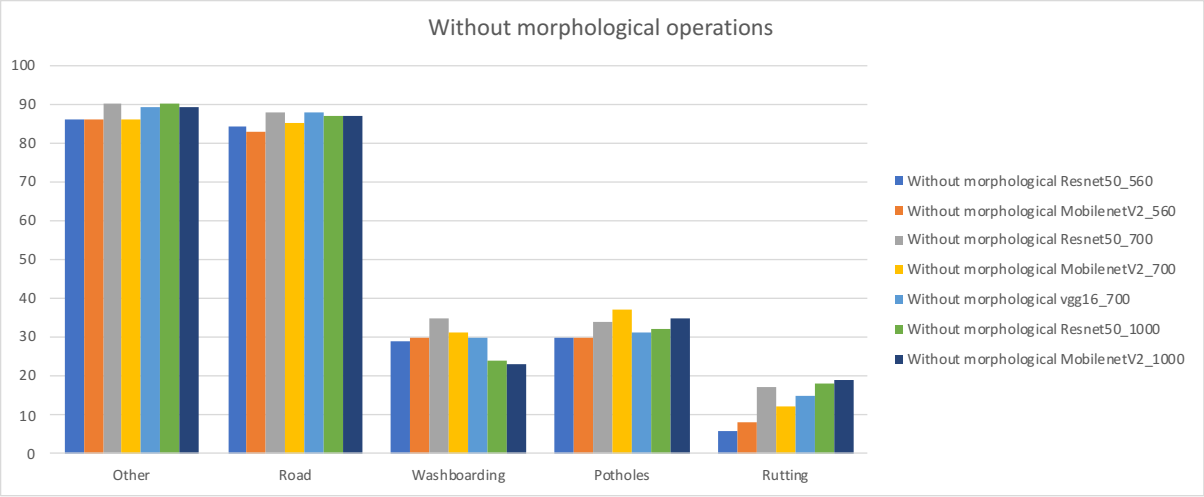

Figure 31: iou DCNN distress detection without morphological operations

The results in Figure 31 show that the iou rates for the "Other" and "Road" classes are rather considerable and are mostly above 83%. Performance of the different DCNN architectures were mostly similar when trained with the same number of training samples, excluding Resnet 50 with 700 images which outperformed the other two classifiers with the same number of training images. Addition of the new training images increased the iou rates for these classes as well. However, the iou results were much lower for the three defect classes and the addition of new training images did not increase the iou results in the Washboarding class.

As mentioned in section 3.5 Testing and postprocessing, post-processing morphological operations were implemented on the binarized segmentation result of each defect class to remove small and isolated noises, and to retain the larger elements. The addition of morphological operations has improved the iou rates of the defect classes by up to 3 percent, even though these improvements are rather small.

Table 5: iou DCNN distress detection with morphological operations

	With morphological						
classes	Resnet50_560	MobilenetV2_560	Resnet50_700	MobilenetV2_700	vgg16_700	Resnet50_1000	MobilenetV2_1000
Other	86	87	90	86	89	90	90
Road	83	83	88	85	88	87	87
Washboarding	31	31	37	34	33	27	27
Potholes	30	30	35	37	32	32	35
Rutting	8	10	20	13	15	19	21

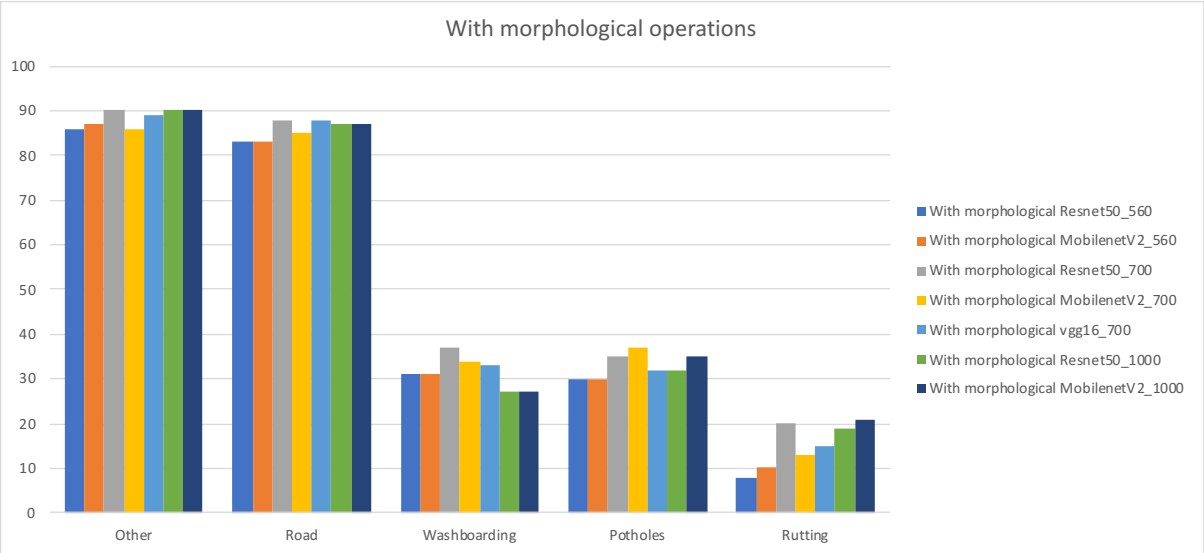

Figure 32: iou DCNN distress detection with morphological operations

4.2 Object level detection

The Object Level Detection approach consists of calculating the DCNN accuracy and precision by using the number of true positives, false positives, and false negatives. The Mobilenetv2 model trained with 1000 images was used to segment the five classes, including other (surrounding), road, pothole washboarding, and rutting, because it was among the best performing classifiers (in all classes except washboarding).

Once the DCNN classifier processed the set of 122 images, the results were compared with the manually labelled images, enabling to spot the true positives, false positives, and false negatives. If a defect segmentation overlapped more than 50% with an actual defect, it was considered as a true positive. The average accuracy and precision rates of the object level detection for the Mobilenetv2 trained with 1000 images on the test images were determined in

two test setups: without morphological and with morphological operations. The results are presented in Table 6 and Figure 33.

Table 6: DCNN accuracy and precision for object level distress detection

	mobilenetv2_1000	
	W/o morphological operations	**W/ morphological operations**
	Accuracy	
Pothole	86%	76%
Washboarding	64%	67%
Rutting	81%	82%
	Precision	
Pothole	53%	67%
Washboarding	42%	47%
Rutting	10%	13%

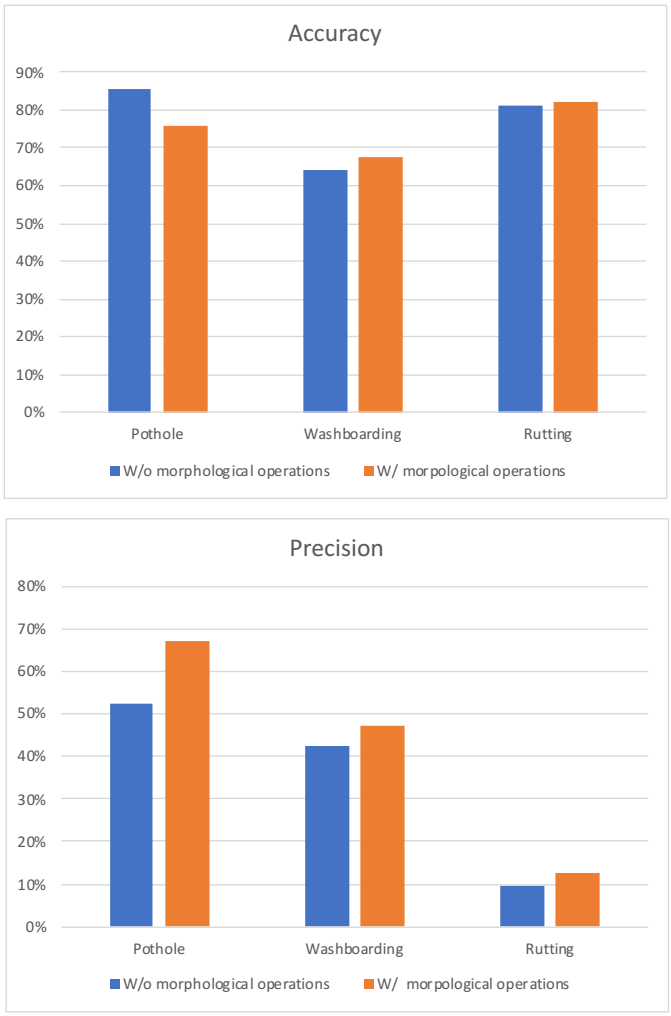

Figure 33: DCNN accuracy and precision for object level distress detection

In the object level analysis, the accuracy rates for the road surface defects, ranged between 64% and 86% without morphological operations, and 67% and 82% with morphological operations in three defect classes. However, for the precision metric, it was found that the “Rutting” class brought the results down to 10% (without morphological operations) and 13% (with morphological operations). It highlights the predominance of false positives found by the DCNN when it comes to rutting., as shown in Figure 34, where the red arrows indicate the spotted false positives for rutting. The vast majority of these false positives were tire tracks which are essentially ruts in nature with very mild depths.

Morphological operations evidently improved precision results in all classes through removal of small patches which were false positives, and also slightly increased the accuracy rates in washboarding and rutting classes. However, morphological operations had a deteriorating effect in the pothole class as they removed some of the small potholes mistaken as small noises. This issue, however, might not a major negative impact on the overall road assessment outcomes, because small potholes are not a main source of concern in common road assessment systems, such as PAVER PMS and Gravel-PASER methods (Eaton et al. 1989; Walker 1991).

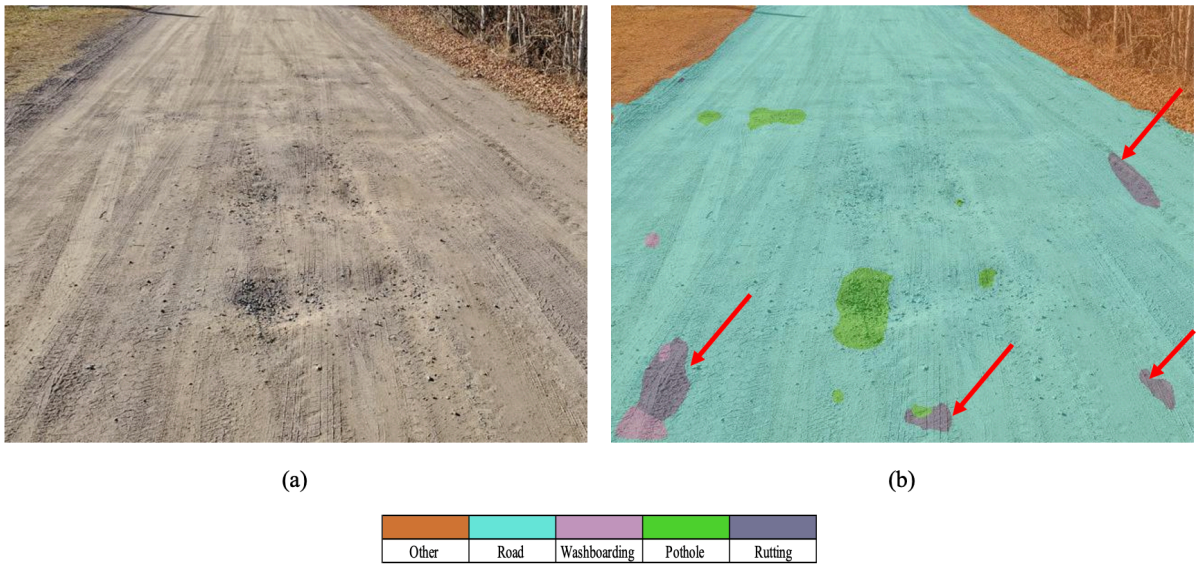

Figure 34: Rutting false positives DCNN detection using mobilenetv2_1000 without morpological operations

4.3 Light deflection over the road surface

The light deflection over the road surface can have a major effect on the appearance of the road surface and its defects. This part of experiments aims to investigate if flying the drone either towards the sunlight or against it would alter the defect detection performance, as shown in Figure 35.

Figure 35: UAV-captured frames of same road segments from opposite directions

Figure 35 shows three sets of images from three same road segments, captured from different directions, including following the sunlight deflection (left side images) and flying against it

(right side images). The first two sets (Figure 35 a. and b., and Figure 35 c. and d). show considerable differences in the appearance of the road and distresses, namely in Figure 35 c. and d., in which the road surface is wet. However, Figure 35 e. and f. were taken in an overcast condition and the visual differences are small.

To develop such comparison, three different unpaved road sections were selected in sunny days and the drone was flown on the same part of the road in opposite directions: one flying towards the light and the second flying against the light. The videos were processed as described in Section 3.2 Data preparation process, where the frames were acquired to be later visually compared and matched, similar to samples presented in Figure 35.

The Mobilenetv2 DCNN model trained with 700 images were used to recognize the defects on the six sets of images. A sample result of segmentations on a corresponding set of frames can be seen in Figure 36.

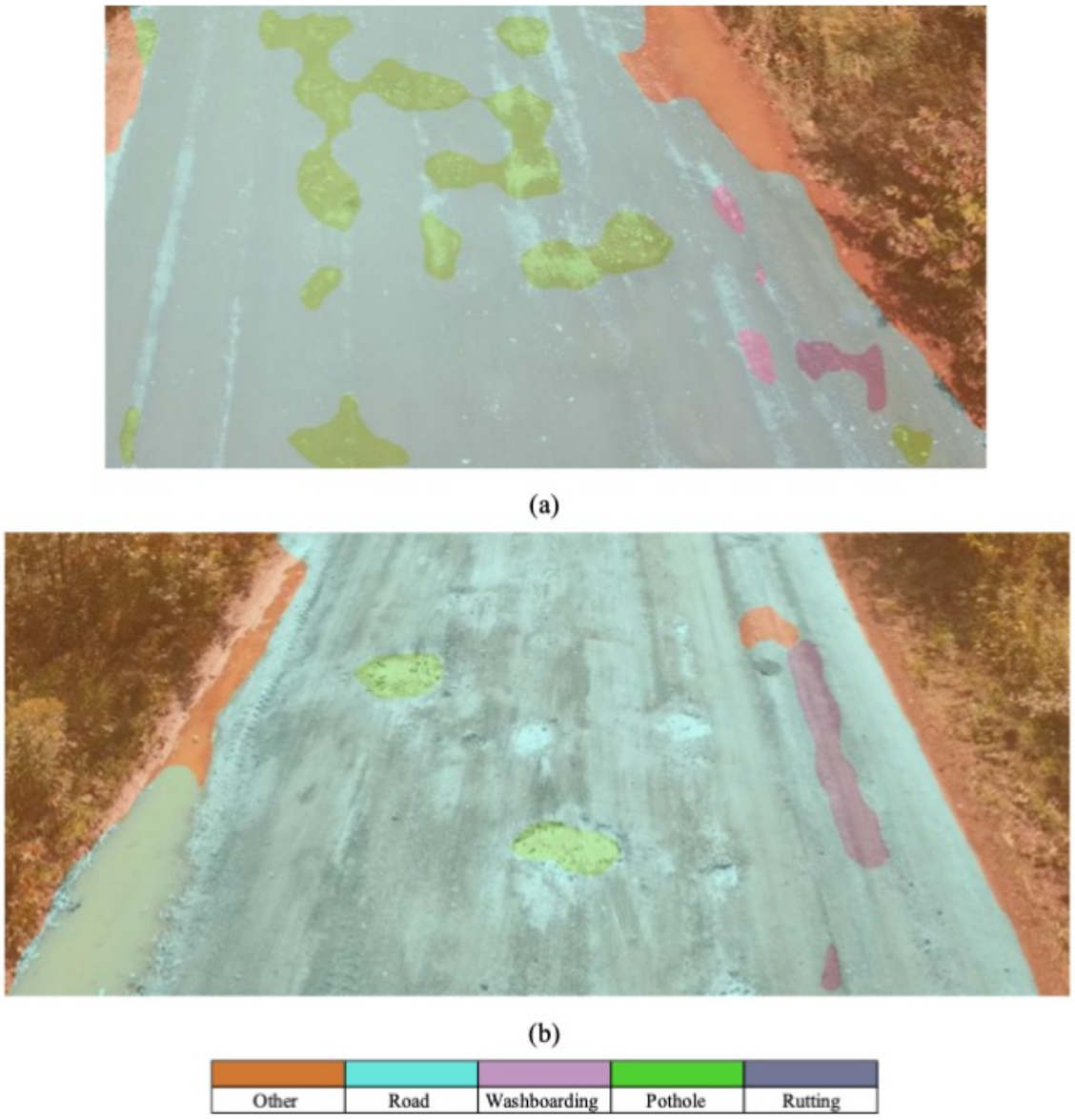

Figure 36: DCNN defect recognition. a) UAV flown towards the light; b) UAV flown against the light

The experiment for assessment of the light deflection analyzed three different road segments, in two opposite directions. Therefore, by applying an object level detection assessment, as proposed in section 4.2 Object level detection, the results were calculated and provided in Table 7.

Table 7: DCNN Accuracy and Precision according to the light deflection

Accuracy		
	Towards the light	Against the light
Pothole	94%	79%
Washboarding	33%	50%

Precision		
	Towards the light	Against the light
Pothole	55%	90%
Washboarding	14%	40%

The "Rutting" class was not considered in this analysis, because it produced too many false positives, as exemplified in Figure 34. It was found that the light deflection may alter the accuracy and precision rates for both pothole and washboarding but not proportionally. While the accuracy for the pothole is greater when the UAV is flown towards the light, for washboarding a better accuracy can be achieved when flying the UAV against the light. On the other hand, better precision rates were achieved when the UAV was flown against the light in both classes. A main reason could be due the contrasting appearance of the defects with the intact road when they exhibit light reflections.

4.4 Defect distribution

Another set of experiments in this research evaluated the possibility of using the developed method to estimate the defect distribution over the road surface. As mentioned in the Chapter 3, it is possible to use the distribution of defects on the road surface in the PASER rating system (Walker 1991), to assess the road surface condition. This was implemented by creating a binary

mask of the road surface and the defect of interest. As described in section 3.6 Defect distribution, case study of potholes, it is possible to determine the percentage of potholes on a specific segment of road surface.

In this set of experiment, the Mobilenetv2 model trained with 1000 coupled with morphological operations was used to estimate the percentage of potholes on the test images and were compared against the percentage obtained from manual labelling. For example, the pothole percentage on the road surface for the example presented on Figure 30, was calculated as follows:

Total pixels: 640 x 480 = 307200

Other (Surrounding) Pixels: 93905

Road pixels: 213295

Pothole pixels: 28795

Pothole distribution on the road surface: $\frac{\#\ \#\text{othole pixels}}{\#\ \text{Road pixels}} = \frac{28795}{213295} = 13{,}5\%$

This assessment was carried out on the test dataset with 122 images and the results of segmentations were compared against the manual labelling. The average of the differences was 2.24% and the standard deviation of the differences was 2.14%. The PASER systems indicates 10% and 25% as thresholds for below Fair and below Poor levels (Table 2), and the differences are in the automated assessment and manual labelling are rather small which highlights the potential of this system for this type of qualitative rating of the road sections.

Figure 37 shows four synthetized samples of the process proposed on Figure 30. It shows the raw image, its DCNN segmentation, and an overlayed image of the binary masks to differ the classes, including “Other (Surrounding)”, “road”, and “Potholes”. Table 8 provides the pothole distribution on the road surface calculated for each test image presented in Figure 37.

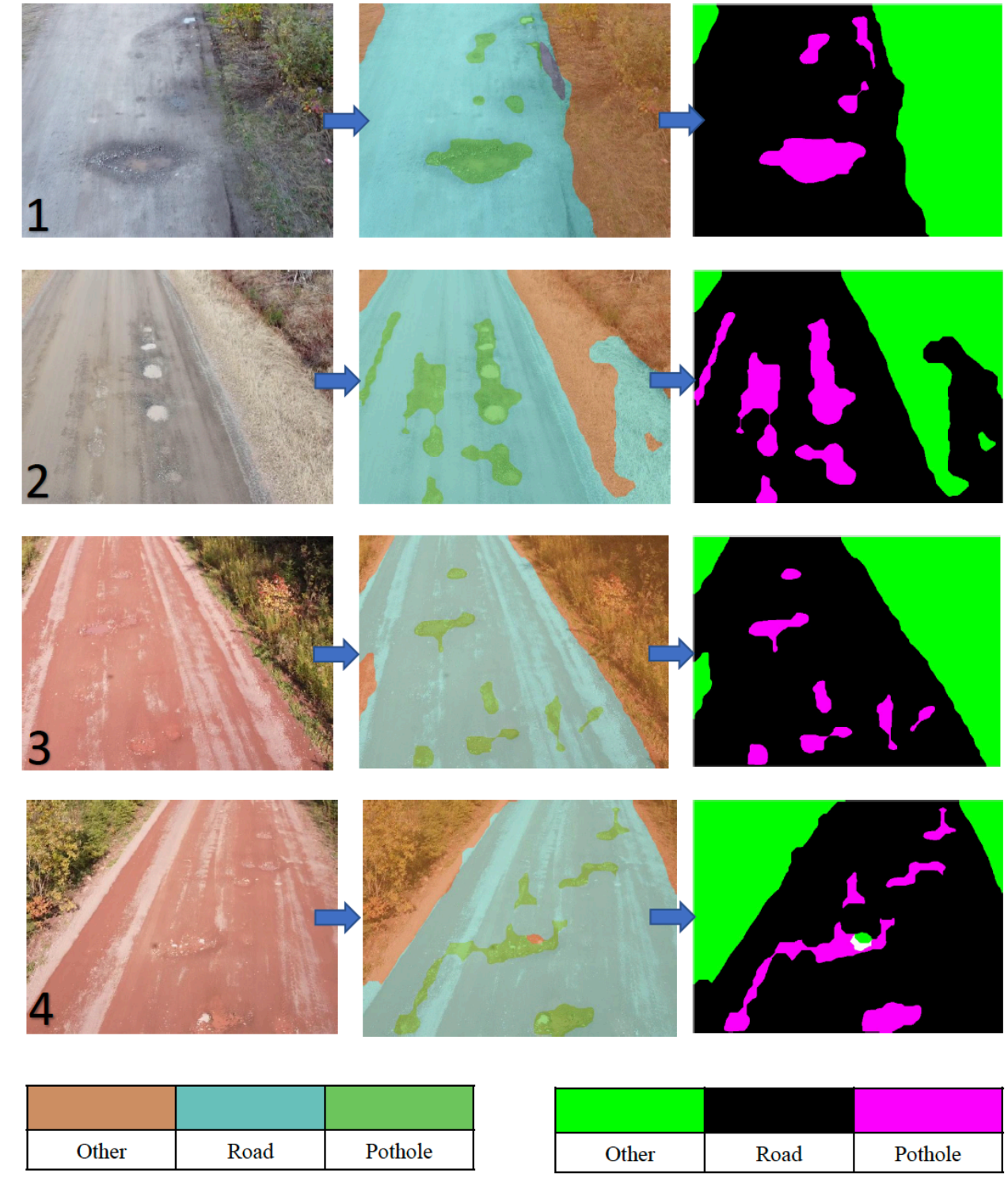

Figure 37: Pothole distribution on four distinct samples from the test dataset

Table 8: Pothole distribution on four distinct samples from the test dataset

Figure 37: image#	1	2	3	4
Defect distribution over the road surface	9%	13%	6%	10%

4.5 Discussion

These test setups were carried out to evaluate the performance of the proposed method and also presented application of the proposed method to an existing unpaved road rating system. The Intersection Over Union (iou) and the object level detection approaches were employed in this research to evaluate the developed classifiers.

The iou approach only measures the overlapping levels between manually labelled images and the DCNN segmentations. This way, it is possible to determine the regions where the detections and actual defects coincide. All the trained DCNN classifiers showed satisfactory performance in segmentation of the road surfaces and surrounding areas with ious ranging from 83% to 90% (Table 5). It is also notable that the increasing of the number of training images increased the iou rates for the surrounding areas and road surface classes.

On the other hand, the results did not present considerable ranges for the iou rates of the road surface defects, as they varied from 27% to 37% for washboarding, 30% to 37% for potholes, and 8% to 21% for rutting (Table 5). Also, increasing of training images did not show a significant increase of iou rates in defect classes.

However, the iou metric might not be the most appropriate measure to objectively assess the performance of the DCNN classifiers, that is because it evaluates on a subject level, accounting for the total area of the defects. For example, it is possible to notice the successful recognition of all the six potholes on the road surface in Figure 38; however, the DCNN recognition

accounts for a greater area than the manually labelled area, resulting in the intersection over union rate of 48%. The outcome of such a subjective analysis highlights the necessity of investigating the proposed method in an objective manner. By applying the object level analysis for the sample presented in Figure 38, the accuracy of 100% and the precision rate of 75% are calculated for the potholes class. Application of this evaluation to the images test set made it possible to have better assessment of the method as presented in Table 6. With this objective analysis, the accuracy rates were between 67% and 82% and precision rates were between 13% and 67%, when morphological operations were applied. The object level approach also presents an issue when observing the performance of the DCNN, it requires a valid threshold to verify the performance of the classifiers. It brings the necessity of validating this method for this research.

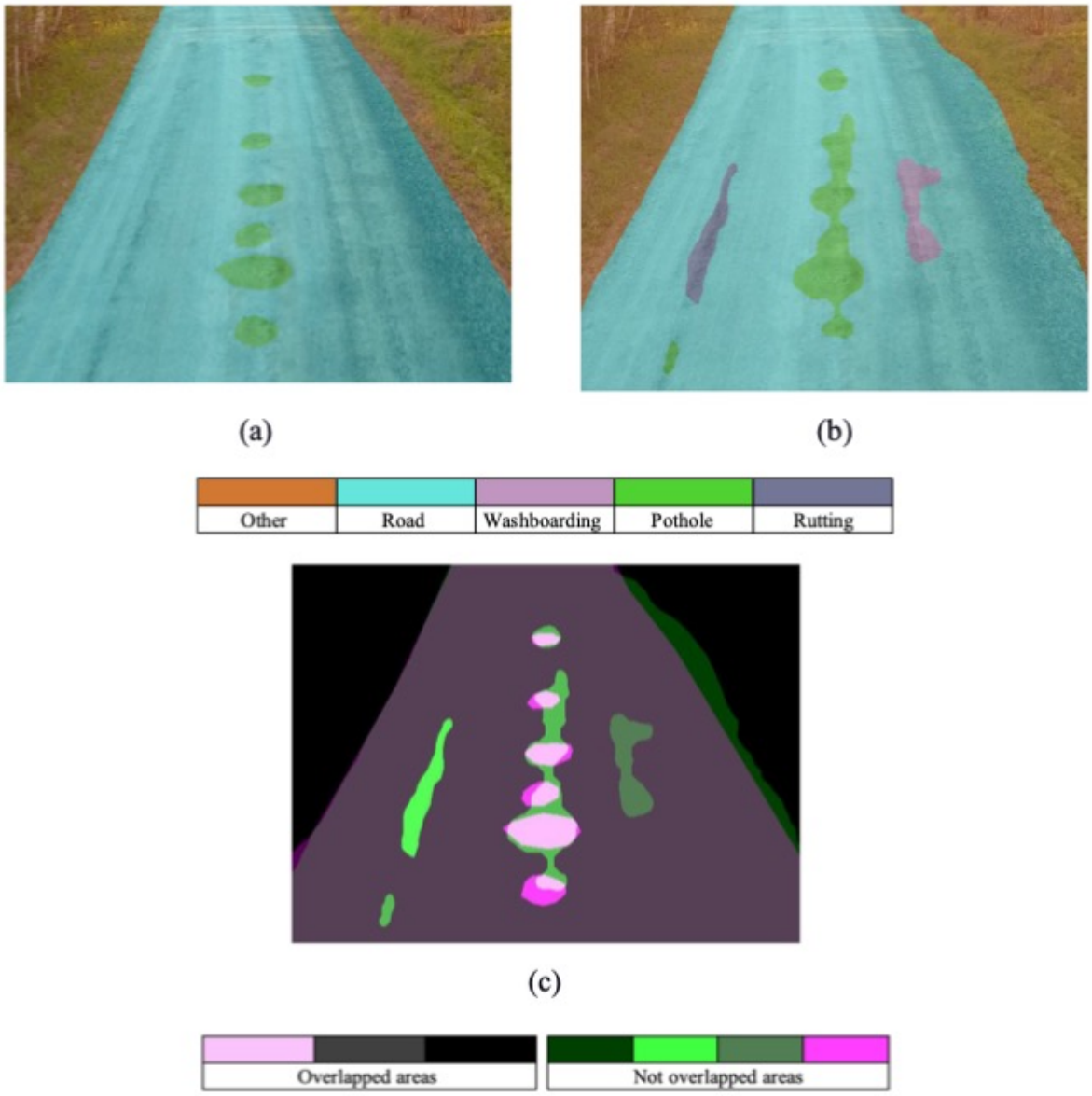

Figure 38: Intersection over union: a) Manually labelled image; b) DCNN-based (mobilenetv2, trained with 1000 images) defect segmentation; c) overlapped areas

Postprocessing the segmentations with morphological operation has shown potential to reduce noises around the road surface area, reduce false positives, and merge the adjacent patches. In particular, the improvements in precision metric are noticeable in Table 6.

Application of morphological operations decreased the accuracy from 85% to 75% in the pothole class. That is because the morphological operations were set up to delete small surrounding noises; therefore, defects smaller than a certain threshold (e.g., 400 pixels) were

deleted from the outcome, as marked with red circles in Figure 39. However, missing the small potholes is not a major problem, because the small-sized scattered potholes are not considered as a serious issue in the unpaved roads rating systems (Walker 1991; Eaton et al. 1989). Since the morphological opening rely on certain size thresholds to remove noises, the future research can look into the dynamic calibration of the thresholds according to the minimum pothole size important in the rating of the roads.

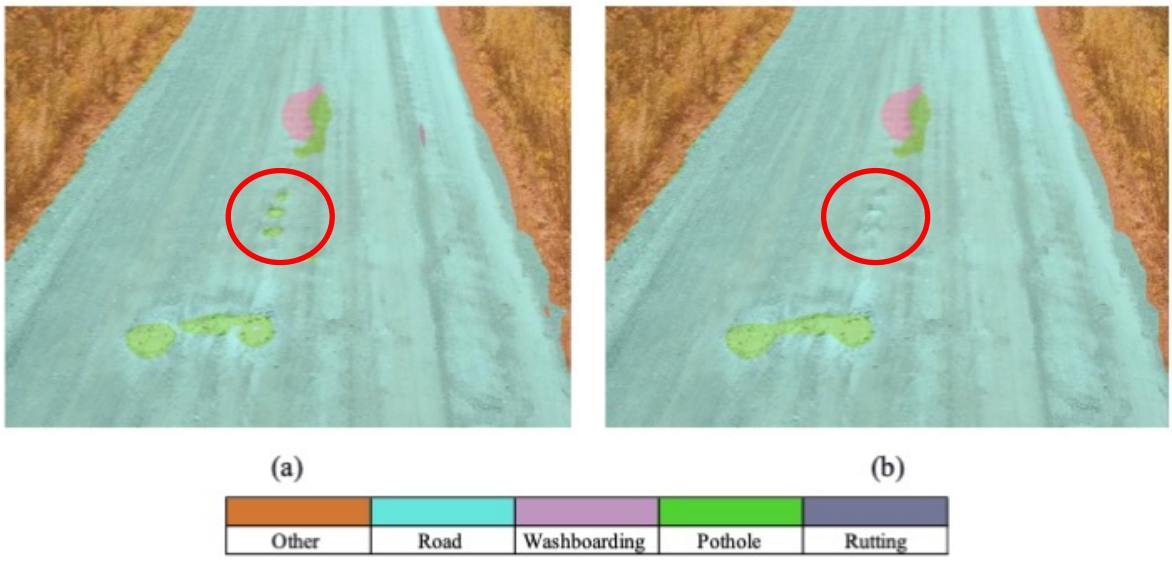

Figure 39: DCNN defect detection using mobilenetv2 trained with 1000 images: a) without morphological operations; b) with morphological operations

4.5.1 Reasons for failures

The obtained results in this research are lower than those achieved using DCNN methods for detection of defects on asphalt roads, including cracks and potholes, which mostly reported accuracy and precision rates over 75% (Mandal et al. 2019; Mei and Gül 2020). The main reason is the difference between the nature of defects on unpaved roads and asphalt roads because cracks and potholes on asphalt roads have distinct visual appearance and texture in images (due to disintegration to the structure of the pavement layer), whereas potholes on unpaved road do not always have a different texture from surrounding areas. For example,

Figure 40 a. shows potholes on a road with distinct visual features which are successfully detected by the classifier; however, Figure 40 c. and Figure 40 e. show potholes (depressions on the road marked by a red circle) on the road surface with minimal visual difference from the surrounding areas and the classifier failed to detect them.

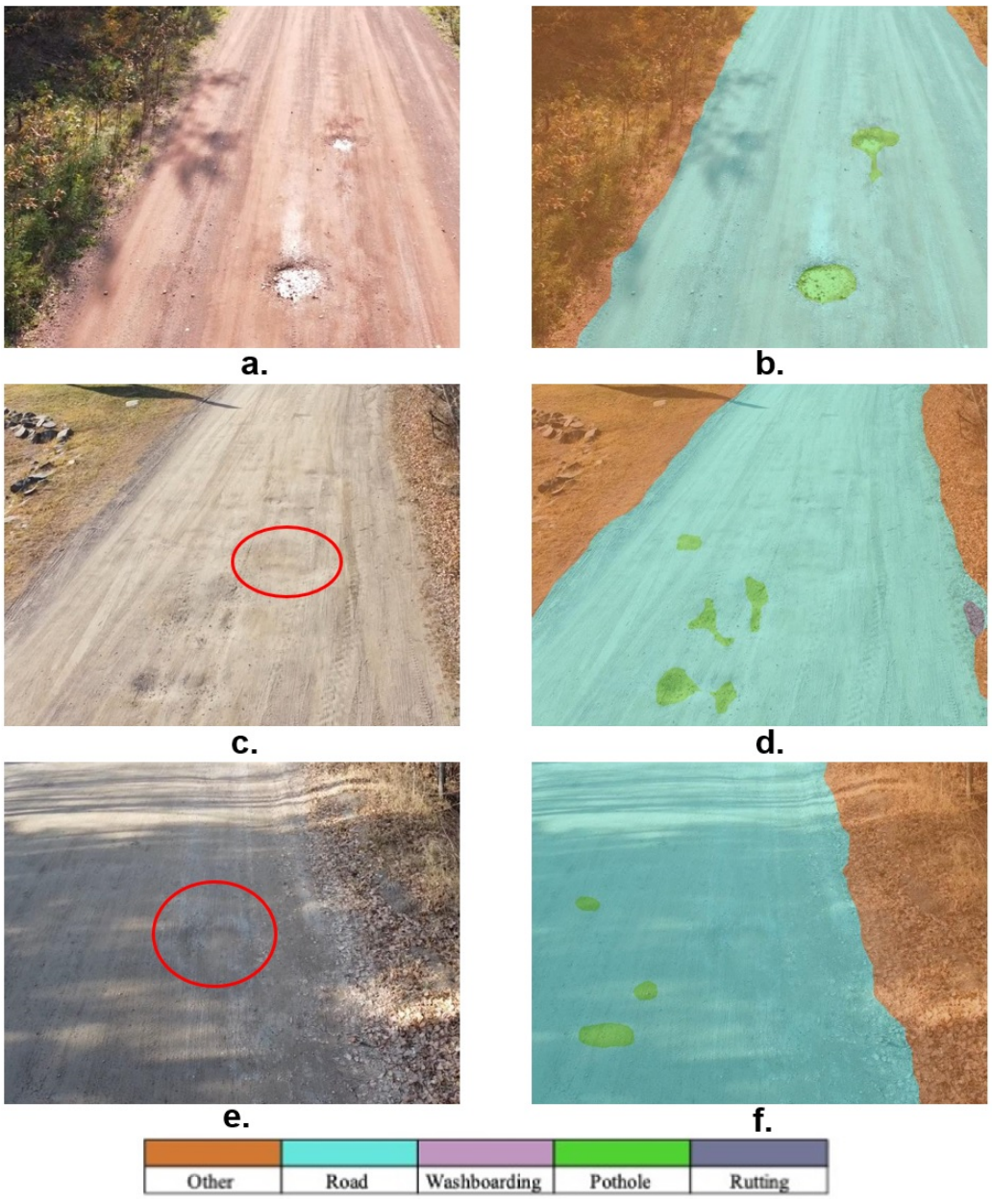

Figure 40: a, c, and e.: three sample UAV-captured frames; b, d, and f.: corresponding segmented frames with morphological operations

There were also noticeable issues with detection of rutting defects. Especially due to their nature, tire tracks or markings on the road surface can be easily misidentified as rutting, that is

because the 2D nature of the images does not allow estimation of the defects' depth, which was the main reason for misidentification of the road markings as rutting samples. Figure 41 a., c., and e., show raw UAV-captured frames where it is possible to spot tire tracks or other marks on the road surface, which were recognized by the mobilenetv2 DCNN, trained with 1000 images, as rutting. However, such recognition could only be verified upon additional analysis of the original video, in which it was possible to verify whether the detected defect was deep enough to be considered as rutting.

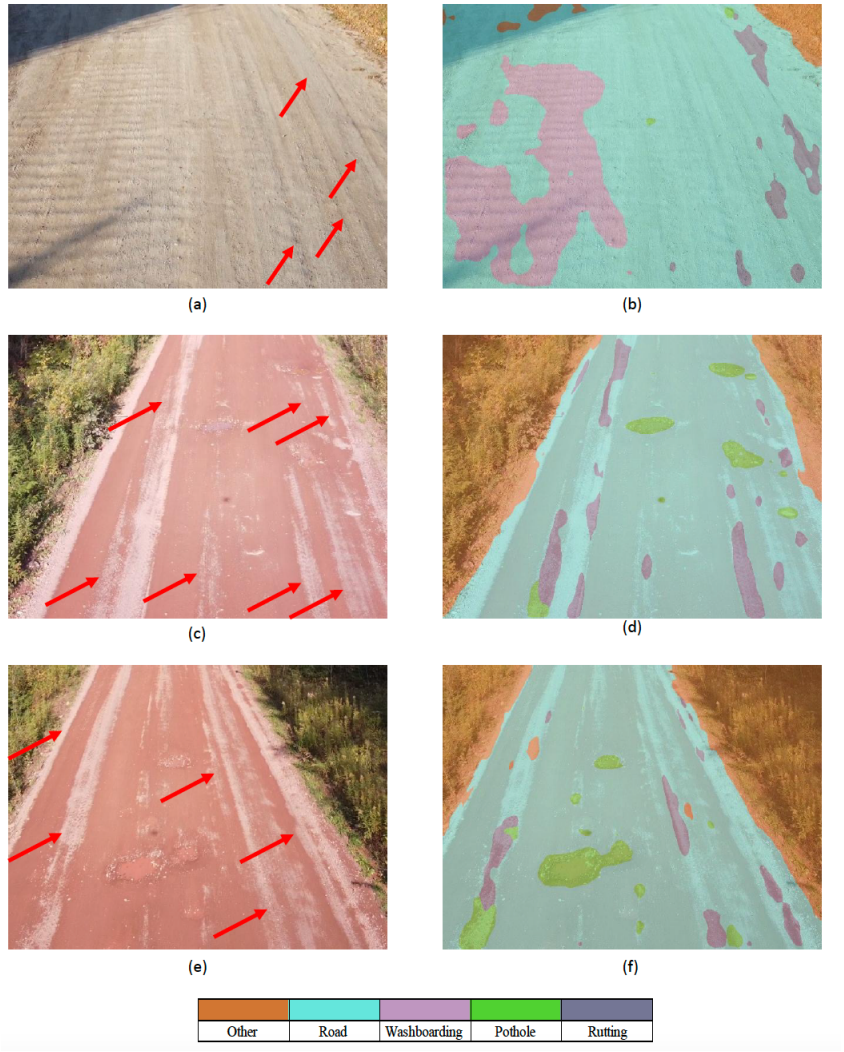

Figure 41: a, c, and e.: three sample UAV-captured frames; b, d, and f.: corresponding segmented frames processed with mobilenetv2_1000

It is possible to spot some flaws as previously mentioned, namely regarding the performance of DCNN defect segmentations. The observed failures were primarily due to the detection of false positives. In order to reach a solid assessment of the performance of this system, there are some points that should be considered.

The first point is the direction in which the UAV is flown: towards or against the light. The frames which were captured when the UAV flew towards the light provided better accuracy rates for the pothole class, and a better precision was achieved when the UAV flew against the light. Washboarding class had greater accuracy and precision rates when the UAV was flown against the light.

The flying parameters of UAV, such as the flight height and the angle set up for capturing images, can interfere and affect the performance of the classifiers, which should be investigated in future.

There is also a question regarding the number of images and instances of each class to be used to train the DCNN classifiers. The results ranged disproportionately to the increase of training images in some cases in this research, which highlighted a question about the optimum number of images and distribution of classes to train the DCNN classifiers to achieve their best performance. Such question opens room for pursuing an optimization problem which will be further investigated.

The last observed point in this research was about the limitations of working with a single 2D image for assessment of a section of the road. During the research process, there were images with defects difficult to recognize, even for human sight, leading to the conclusion that colours, textures, and shades can affect the performance of the system. These items support the idea of capturing images in different heights and angles for training purposes and pursuing methods for 3D analysis of the detected defects.

Chapter 5: Conclusion

5.1 Summary

A computer vision-based system was developed to automatically detect defects and evaluate their extent on the unpaved roads surfaces. The proposed system is part of a larger study, which aims to automate the assessment of defects on unpaved roads networks.

The presented research effort consists of two main parts. First part studied the use of an UAV to collect videos from the distressed roads surface. Second part investigated the use of a cutting-edge machine learning approach, known as deep learning, to detect and assess the defects in the collected video frames.

Although this research project primarily relied on two main steps, the breakdown for the development of the proposed system goes further into more details. It included training of different pre-trained DCNN classifiers. Then the trained DCNN models were tested using a distinct set of images. An investigation of the obtained results led to development of a post-processing algorithm, which consists of morphological operations to mitigate the presence of noises, such as small false positives, and merging adjacent segmented particles.

The trained DCNN classifiers and addition of postprocessing method were tested using two approaches: (1) The first testing approach assessed the overlapping of the segmented test images with the manually labelled defects, creating an area of intersection when the segmentations matched. (2) The second method evaluated the accuracy and precision of the results on the object level. The comparison between these methods allowed to find a practical analysis suited for the purposes of unpaved road condition assessment. Moreover, the effect of light deflection on the road images was assessed. The aim of this evaluation was to find the UAV flight direction with respect to the sunlight to obtain better results. Finally, the proposed

defect segmentation method was applied to an already exiting unpaved road assessment and evaluation systems.

5.2 Conclusions

Detailed observation of the results showed promising performance of the developed system in detection of potholes and washboarding defects. However, it did not provide suitable outcome for the rutting defects, as the method produced too many false positives, which is believed to be due to their appearance in the images which could be similar to other longitudinal markings on the road, namely tire tracks. The optimal outcome of this study was obtained in potholes and washboarding classes due to their distinct appearance in 2D images. Moreover, addition of the postprocessing method has shown considerable potential in reducing false positives and thereby improving the precision of the results; however, it negatively affected the accuracy of the pothole detection results due to possible removal of small potholes.

The proposed system has shown potential to integrate into an already existing system, such as PASER rating system and treatment measurements (Walker 1991).

Although the system did not present great accuracy for rutting, in neither Intersection Over Union (iou) nor Object Level, there are opportunities for future investigations which will be discussed later in this chapter.

5.3 Limitations

The main limitations of the proposed system are provided below:

- Due to weather conditions in Canada, there is a limited time window (Spring/Summer) that it is possible to collect data.
- Since training DCNN classifiers require massive computation power for training (e.g., multicore GPUs), the training images should be resized to reduce required

computational power, which can make some defect instances harder to identify even at human sight.

- Colour of the road surface had some effect on the performance of the classifiers. for example, road surfaces with a gray background were more problematic compared to the roads with red/brown (clay) background.
- The proposed method was developed to process 2D images; however, this does not allow estimation of the defects' depth, which is an important factor in assessment of defects in unpaved roads.

5.4 Recommendation for future work

There are some recommendations for future research projects to advance this study:

- Investigate how the UAV flight and imaging parameters (such as height and camera angle) can affect the DCNN detection results.
- Apply optimization algorithms to determine the optimum number of images and frequency of class samples required to train a DCNN classifier with satisfactory results.
- Investigate automated UAV flight control based on the real-time segmentation of the road path in the captured video frames.
- Investigate method for 3D depth estimation of the detected defects on the unpaved roads.
- Investigate acceptable accuracy and precision levels for the object detection analysis.

References

Alhasan, A., White, D. J., and De Brabanter, K. (2015). "Quantifying Roughness of Unpaved Roads by Terrestrial Laser Scanning." *Transportation Research Record: Journal of the Transportation Research Board*, 2523(1), 105–114.

Aparna, Bhatia, Y., Rai, R., Gupta, V., Aggarwal, N., and Akula, A. (2019). "Convolutional neural networks-based potholes detection using thermal imaging." *Journal of King Saud University - Computer and Information Sciences*.

Archondo-Callao, R. S. (1999). "Unpaved Roads'Roughness Estimation by Subjective Evaluation." *Infrastructure Notes Transport, Water and Urban Development. The World Bank.*, 2–4.

Archondo-callao, R. (2004). "Economically Justified Levels of Road Works Expenditures on Unpaved Roads." *Transport Notes Series; No.TRN 2. World Bank, Washington, DC. © World Bank.*

Butcher, J. B., Day, C. R., Austin, J. C., Haycock, P. W., Verstraeten, D., and Schrauwen, B. (2014). "Defect detection in reinforced concrete using random neural architectures." *Computer-Aided Civil and Infrastructure Engineering*, 29(3), 191–207.

Cambridge Systematics, Inc., and Meyer, M. D. (2007). "Best Practices in Transportation Asset Management." Nchrp 20-68, (U.S. Domestic Scan Program).

Cao, M. T., Tran, Q. V., Nguyen, N. M., & Chang, K. T. (2020). Survey on performance of deep learning models for detecting road damages using multiple dashcam image resources. *Advanced Engineering Informatics*, *46*(April), 101182. https://doi.org/10.1016/j.aei.2020.101182

Central Intelligence Agency (2021) "Roadways" <https://www.cia.gov/the-world-factbook/field/roadways/>, accessed May 30, 2021

Chun, C., and Ryu, S.-K. (2019). “Road Surface Damage Detection Using Fully Convolutional Neural Networks and Semi-Supervised Learning.” *Sensors*, 19(24), 5501.

Da-Jiang Innovations. (2021). “Mavic Mini.” <https://www.dji.com/ca/mavic-mini?site=brandsite&from=nav> (Apr. 5, 2021).

Da-Jiang Innovations. (2021). “Mavic Mini - Specifications - DJI Professional.” <https://www.dji.com/ca/mavic-mini/specs> (Mar. 25, 2021).

DeepLizard. (2019). “Convolutional Neural Networks (CNNs) Explained.” *Deep Learning Course 1 of 4 - Level: Beginner*, Apress, Berkeley, CA, <https://deeplizard.com/learn/video/YRhxdVk_sIs> (Mar. 23, 2021).

Dobson, R. J., Brooks, C., Roussi, C., and Colling, T. (2013). “Developing an unpaved road assessment system for practical deployment with high-resolution optical data collection using a helicopter UAV.” *2013 International Conference on Unmanned Aircraft Systems, ICUAS 2013 - Conference Proceedings*, IEEE, 235–243.

Doycheva, K., Koch, C., and König, M. (2016). “GPU-enabled pavement distress image classification in real time.” Journal of Computing in Civil Engineering, 31(3), 04016061.

Dung, C. V. and Anh, L.D. (2019). “Autonomous concrete crack detection using deep fully convolutional neural network.” Automation in Construction, 99, 52-58.

Eaton, R. A., Gerard, S., and Dattilo, R. S. (1989). “Method for rating unsurfaced roads.” The Northern engineer, 21(1–2), 30–40.

Government of Canada. (n.d.). “Transportation in Canada. Highways.” <http://www.tc.gc.ca/eng/policy/acg-acgd-menu-highways-2141.htm >.

Harikrishnan, P. M., and Gopi, V. P. (2017). “Vehicle Vibration Signal Processing for Road Surface Monitoring.” *IEEE Sensors Journal*, 17(16), 5192–5197.

He, K., Zhang, X., Ren, S., and Sun, J. (2016). “Deep Residual Learning for Image Recognition.” *2016 IEEE Conference on Computer Vision and Pattern Recognition (CVPR)*, IEEE, 770–778.

Henrique Oliveira, P. L. C. (2009). “Automatic Road Crack Segmentation Using Entropy and Image Dynamic Thresholding.” *17th European Signal Processing Conference (EUSIPCO 2009)*, 63(3), 1066–1071.

Hoang, N. D., Nguyen, Q. L., and Tien Bui, D. (2018). “Image Processing-Based Classification of Asphalt Pavement Cracks Using Support Vector Machine Optimized by Artificial Bee Colony.” *Journal of Computing in Civil Engineering*, 32(5).

Howard, A. G., Zhu, M., Chen, B., Kalenichenko, D., Wang, W., Weyand, T., Andreetto, M., and Adam, H. (2017). “MobileNets: Efficient Convolutional Neural Networks for Mobile Vision Applications.” *arXiv*.

Huntington, G., and Ksaibati, K. (2009). “Annualized road works cost estimates for unpaved roads.” Journal of Transportation Engineering, 135(10), 702–710.

ImageNet. (2020). Accessed July 24, 2020. http://www.image-net.org

Jahren Charles, Z. Z. (2015). *Aggregate Road Surface Rejuvenation*.

Koch, C., Georgieva, K., Kasireddy, V., Akinci, B., and Fieguth, P. (2015). “A review on computer vision-based defect detection and condition assessment of concrete and asphalt civil infrastructure.” *Advanced Engineering Informatics*, Elsevier Ltd, 29(2), 196–210.

Li, B., Wang, K. C., Zhang, A., Yang, E., and Wang, G. (2020). “Automatic classification of pavement crack using deep convolutional neural network.” International Journal of Pavement Engineering, 21(4), 457-463.

Liu, J., Yang, X., Lau, S., Wang, X., Luo, S., Lee, V. C.-S., and Ding, L. (2020). Automated pavement crack detection and segmentation based on two-step convolutional neural network. Computer-Aided Civil and Infrastructure Engineering, 35(11), 1291–1305.

Maine Department of Environmental Protection. (2016). “A Guide for Landowners on Camp and Other Gravel Roads.” *Gravel Road Maintenance Manual*, (April).

Mandal, V., Uong, L., and Adu-Gyamfi, Y. (2019). “Automated Road Crack Detection Using Deep Convolutional Neural Networks.” Proceedings - 2018 IEEE International Conference on Big Data, Big Data 2018, IEEE, 5212–5215.

Marra, E., Wictorsson, R., Bohlin, J., Marchi, E., and Nordfjell, T. (2021). Remote measuring of the depth of wheel ruts in forest terrain using a drone. International Journal of Forest Engineering, 1-11.

Mathworks. (2019). “Pretrained Deep Neural Networks.” <https://www.mathworks.com/help/deeplearning/ug/pretrained-convolutional-neural-networks.html> (Mar. 19, 2021).

MATLAB. (2017). “Pretrained VGG-16 convolutional neural network - MATLAB vgg16.” <https://www.mathworks.com/help/deeplearning/ref/vgg16.html> (Mar. 24, 2021).

MATLAB & Simulink. (2021). “Convolutional Neural Network 3 things you need to know.” <https://www.mathworks.com/discovery/convolutional-neural-network-matlab.html?s_tid=srchtitle> (Mar. 19, 2021).

McLaughlin, E., Charron, N., & Narasimhan, S. (2020). Automated defect quantification in concrete bridges using robotics and deep learning. Journal of Computing in Civil Engineering, 34(5), 04020029.

Mei, Q., and Gül, M. (2020). “A cost-effective solution for pavement crack inspection using cameras and deep neural networks.” Construction and Building Materials, Elsevier, 256, 119397.

Nasiruddin Khilji, T., Lopes Amaral Loures, L., & Rezazadeh Azar, E. (2021). Distress Recognition in Unpaved Roads Using Unmanned Aerial Systems and Deep Learning

Segmentation. *Journal of Computing in Civil Engineering*, *35*(2), 04020061. https://doi.org/10.1061/(ASCE)CP.1943-5487.0000952

Oransi. (2021). "Dust from Roads and Your Respiratory Health." <https://www.oransi.com/page/dust-roads-your-respiratory-health> (Sep. 17, 2021).

Pan, S. J., and Yang, Q. (2009). "A survey on transfer learning." IEEE Transactions on knowledge and data engineering, 22(10), 1345-1359.

Pan, Y., Zhang, X., Cervone, G., and Yang, L. (2018). "Detection of Asphalt Pavement Potholes and Cracks Based on the Unmanned Aerial Vehicle Multispectral Imagery." IEEE Journal of Selected Topics in Applied Earth Observations and Remote Sensing, IEEE, 11(10), 3701–3712.

Pei, L., Shi, L., Sun, Z., Li, W., Gao, Y., and Chen, Y. (2021). Detecting Potholes in Asphalt Pavement under Small-sample Conditions Based on Improved Faster Region-based Convolution Neural Networks. Canadian Journal of Civil Engineering, (ja).

Pereira, V., Tamura, S., Hayamizu, S., and Fukai, H. (2018). "Classification of Paved and Unpaved Road Image Using Convolutional Neural Network for Road Condition Inspection System." In 2018 5th International Conference on Advanced Informatics: Concept Theory and Applications (ICAICTA), 165-169. IEEE.

Radopoulou, S. C., and Brilakis, I. (2015). "Patch detection for pavement assessment." Automation in Construction, 53, 95-104.

Rawat, W., and Wang, Z. (2017). "Deep Convolutional Neural Networks for Image Classification: A Comprehensive Review." *Neural Computation*, 29(9), 2352–2449.

Saeed, N., Dougherty, M., Nyberg, R. G., Rebreyend, P., and Jomaa, D. (2020). A Review of Intelligent Methods for Unpaved Roads Condition Assessment. In 2020 15th IEEE Conference on Industrial Electronics and Applications (ICIEA) (pp. 79-84). IEEE.

Sahari Moghaddam, A., Rezazadeh Azar, E., Mejias, Y., and Bell, H. (2020). "Estimating Stripping of Asphalt Coating Using k-Means Clustering and Machine Learning–Based Classification." Journal of Computing in Civil Engineering, 34(1), 04019044.

Sandler, M., Howard, A., Zhu, M., Zhmoginov, A., and Chen, L. C. (2018). "Mobilenetv2: Inverted residuals and linear bottlenecks." In Proceedings of the IEEE Conference on Computer Vision and Pattern Recognition, 4510-4520.

Sattar, Shahram, Songnian Li, and Michael Chapman. (2018). Road surface monitoring using smartphone sensors: A review. Sensors 18(11), 3845.

Sayers, M. W., Gillespie, T. D., and Paterson, W. D. O. (1986). *Guidelines for Conducting and Calibrating Road Roughness Measurements*. *World Bank Technical Paper Number 46*.

Sayers, M. W., and Karamihas, S. M. (1998). *The Little Book of Profiling*. *University of Michigan*. < http://www.umtri.umich.edu/content/LittleBook98R.pdf>.

Simonyan, K., and Zisserman, A. (2014). "Very Deep Convolutional Networks for Large-Scale Image Recognition." *3rd International Conference on Learning Representations, ICLR 2015 - Conference Track Proceedings*, 1–14.

Song, H., Baek, K., and Byun, Y. (2018). "Pothole Detection using Machine Learning." *Advanced Science and Technology*, 151–155.

Szegedy, C., Liu, W., Jia, Y., Sermanet, P., Reed, S., Anguelov, D., Erhan, D., Vanhoucke, V., and Rabinovich, A. (2015). "Going deeper with convolutions." *Proceedings of the IEEE Computer Society Conference on Computer Vision and Pattern Recognition*, 07-12-June-2015, 1–9.

Tariq Ahmad. (2014). *National Funding of Road Infrastructure: Canada*. Library of Congress. https://www.loc.gov/law/help/infrastructure-funding/canada.php#_ftnref4

Transport Canada. (2020). “Flying your drone safely and legally.” <https://tc.canada.ca/en/aviation/drone-safety/flying-your-drone-safely-legally#legal> (Mar. 25, 2021).

Transport Canada. (2019). “New rules for drones in Canada.” <https://tc.canada.ca/en/aviation/drone-safety/new-rules-drones-canada>.

Transport Canada. (2018). *Transportation in Canada 2018 Overview Report*. <https://www.tc.gc.ca/eng/policy/transportation-canada-2018.html#item-10>

Transport Canada. (2021). “Highways.” <https://tc.canada.ca/en/corporate-services/policies/highways> (Aug. 15, 2021).

Walker, D. M. (1991). “Evaluation and rating of gravel roads.” *Transportation Research Record*, 1291 (Vol., 121–125.

Walker, D. (2002). *Pavement Surface Evaluation and Rating Gravel PASER Manual*.

Wu, W., Qurishee, M. A., Owino, J., Fomunung, I., Onyango, M., and Atolagbe, B. (2019). “Coupling Deep Learning and UAV for Infrastructure Condition Assessment Automation.” *2018 IEEE International Smart Cities Conference, ISC2 2018*, IEEE, 1–7.

Yamada, T., Ito, T., and Ohya, A. (2013). “Detection of road surface damage using mobile robot equipped with 2D laser scanner.” *Proceedings of the 2013 IEEE/SICE International Symposium on System Integration*, IEEE, 250–256.

Yang, Q., & Ji, X. (2021). *Automatic Pixel-level Crack Detection for Civil Infrastructure Using Unet++ and Deep Transfer Learning. IEEE Sensors Journal.*

Ye, W., Jiang, W., Tong, Z., Yuan, D., and Xiao, J. (2019). “Convolutional neural network for pothole detection in asphalt pavement.” Road Materials and Pavement Design, 1-17.

Zhang, C. (2010). “Monitoring the condition of unpaved roads with remote sensing and other technology.” *Final Report US DOT DTPH56-06-BAA-0002*, 1–53.

Zhang, C., and Elaksher, A. (2012). “An unmanned aerial vehicle-based imaging system for 3D measurement of unpaved road surface distresses.” *Computer-Aided Civil and Infrastructure Engineering*, 27(2), 118–129.

Appendix

Data preparation process – MATLAB Code

```
clear all, close all, clc;


vid=VideoReader('/Users/llopesa/Desktop/Videos/DJI_0001.MP4');


numFrames = vid.NumberOfFrames;
n=numFrames;


for i = 1:n
  if mod(i,120) == 0
     frame = read(vid,i);
     image = imcrop(frame, [460, 330, 999, 749]);
     im2=imresize(image, [300 400]);
     imwrite(im2 ,['/Users/llopesa/Desktop/Videos/Frames/' int2str(1), '.jpg']);
  end
end
```

Training process using the pre-trained neural networks – MATLAB Code

```
clear all; close all; clc;


load("C:\Users\ehsan\Desktop\Luana\gTruth.mat")
imds = imageDatastore('C:\Users\ehsan\Desktop\Luana\Defect Images');
pxds = pixelLabelDatastore(gTruth);
classes = pxds.ClassNames;
```

```
cmap1 = [
            120 120 50    % 1
            100 250 240     % 2
            192 150 122   % 3
            80 70 180       % 4
            55 90  190      % 5
];
cmap1 = cmap1 ./ 255;

I = readimage(imds, 20);
C = readimage(pxds,20);
B = labeloverlay(I,C,'ColorMap',cmap1);
imshow(B);
pixelLabelColorbar(cmap1,classes);

%% training preparation
imageSize = [300 400 3];

% Specify the number of classes.
numClasses = numel(classes);

% Create Segnet Layers
lgraph = segnetLayers(imageSize, numClasses, 'vgg16');
%% lgraph = deeplabv3plusLayers(imageSize, numClasses, "mobilenetv2");

options = trainingOptions('sgdm', ...
    'Momentum', 0.9, ...
    'InitialLearnRate', 1e-2, ...
```

```
    'L2Regularization', 0.0005, ...
    'MaxEpochs', 120, ...
    'MiniBatchSize', 4, ...
    'Shuffle','every-epoch', ...
    'CheckpointPath', tempdir,...
    'Verbose', false,...
    'Plots','training-progress');


augmenter = imageDataAugmenter('RandXReflection',true,...
    'RandXTranslation',[-10 10], 'RandYTranslation' ,[-10 10]);
datasource = pixelLabelImageDatastore(imds, pxds, ...
    'DataAugmentation',augmenter);


%%%% start training
tic
[net, info] = trainNetwork(datasource, lgraph, options);
toc
save('C:\Users\Ehsan\Desktop\Tanzim\PreTrainedCNN.mat', 'net', 'info', 'options');
disp('NN trained');
%%%% end training
```

Defect Recognition with DCNN -MATLAB Code

```
clear all; close all; clc;


load ("/Users/llopesa/Desktop/Research/Test/Labeled Images/gTruth_1");
imdsTest = imageDatastore('/Users/llopesa/Desktop/Research/Test/Images');
pxdsTest = pixelLabelDatastore(gTruth);
classes = pxdsTest.ClassNames;
```

```
cmap1 = [
            210 120 50    % 1
            100 230 220     % 2
            192 150 192   % 3
            80 210 50       % 4
            115 118 150       % 5
];
cmap1 = cmap1 ./ 255;


I = readimage(imdsTest, 1);


data = load('/Users/llopesa/Desktop/Research/Test/700_images_classifiers/resnet50');
net = data.net;
C = semanticseg(I, net);
B = labeloverlay(I,C,'Colormap',cmap1,'Transparency',0.4);
pixelLabelColorbar(cmap1,classes);


expectedResult = readimage(pxdsTest, 1);
actual = uint8(C);
expected = uint8(expectedResult);
imshowpair(actual, expected)


iou = jaccard(C,expectedResult);
table(classes,iou)


for j = 1:100
   I = readimage(imdsTest, j);
   C = semanticseg(I, net);
   expectedResult = readimage(pxdsTest, j);
```

```
  iou = jaccard(C,expectedResult);
  j
  table(classes,iou)
end


pxdsResults = semanticseg(imdsTest,net, ...
   'MiniBatchSize',1, ...
   'WriteLocation',tempdir, ...
   'Verbose',false);
metrics = evaluateSemanticSegmentation(pxdsResults,pxdsTest,'Verbose',false);
metrics.DataSetMetrics
metrics.ClassMetrics
```

Road Segmentation with DCNN – MATLAB Code

```
clear all; close all; clc;


imdsTest = imageDatastore('C:\Users\Luana-PC\Desktop\Research\Test_videos\Images\A2');
data = load('C:\Users\Luana-PC\Desktop\Research\Test_videos\CNN_mobilenetv2_2.mat');
net = data.net;


for j = 1:32
   ILarge = readimage(imdsTest, j);
   I = imresize(ILarge, 0.5);


   C = semanticseg(I, net);
   [rows, columns, Channels] = size(I);
   TempIm = zeros(rows, columns, 1, 'uint8');
```

```
    BW = zeros(rows, columns, 1, 'logical');
    BW(C=='UnpavedRoad') = 1;
    BW2 = bwareaopen(BW,25);

    se = strel('disk',20);
    closeBW = imclose(BW2,se);

    CC = bwconncomp(closeBW);
    numPixels = cellfun(@numel,CC.PixelIdxList);
    [biggest,idx] = max(numPixels);
    BW2 = zeros(rows, columns, 1, 'logical');
    BW2(CC.PixelIdxList{idx}) = 1;

    TempIm(BW2==1) = 255;

    info = regionprops(BW2,'Boundingbox') ;
    BB = info(1).BoundingBox;

    image2 = imcrop(ILarge, [BB(1)*2, rows, BB(3)*2, rows-1]);
    imwrite(image2, ['C:\Users\Luana-PC\Desktop\Research\Test_videos\Images\A2\Segmented\A2_'
num2str(j) '.jpg']);
end
```

Defect Recognition without morphological operation – MATLAB Code

```
clear all; close all; clc;

imdsTest = imageDatastore('/Users/llopesa/Desktop/Research/Test_videos/Images/A2/Segmented');
cmap1 = [
```

```
            210 120 50    % 1
            100 230 220     % 2
            192 150 192   % 3
            80 210 50       % 4
            115 118 150       % 5
];
cmap1 = cmap1 ./ 255;


data = load('/Users/llopesa/Desktop/Research/Test/resnet50');
net = data.net;


for j=1:32
  ILarge = readimage(imdsTest, j);
  I = imresize(ILarge, 0.7);
  C = semanticseg(I, net);
  B = labeloverlay(I,C,'Colormap',cmap1,'Transparency',0.5);
  imwrite(B, ['/Users/llopesa/Desktop/Research/Test_videos/Images/A2/Distress_A2/A2_' num2str(j) '.jpg']);
end
```

Defect Recognition with morphological operation – MATLAB Code

```
clear all; close all; clc;


imdsTest = imageDatastore('…\Images\A2\Segmented');
cmap1 = [
            210 120 50    % 1
            100 230 220     % 2
            192 150 192   % 3
            80 210 50       % 4
            115 118 150       % 5
```

```
];
cmap1 = cmap1 ./ 255;


data = load('…\Test\resnet50');
net = data.net;


for j=1:32
  ILarge = readimage(imdsTest, j);
  I = imresize(ILarge, 0.7);
  C = semanticseg(I, net);
  [rows, columns, Channels] = size(I);
  C2 = C;
  C2(C=='Other' | C=='Road' | C=='Potholes' | C=='Rutting' | C=='Washboarding' ) = 'Road';


   BW1 = zeros(rows, columns, 1, 'logical');
   BW1(C=='Potholes') = 1;
   BW1 = bwareaopen(BW1,400);
   se = strel('disk', 15);
   closeBW1 = imclose(BW1,se);
   C2(closeBW1==1) = 'Potholes';


   BW1 = zeros(rows, columns, 1, 'logical');
   BW1(C=='Rutting') = 1;
   BW1 = bwareaopen(BW1,400);
   se = strel('disk', 15);
   closeBW1 = imclose(BW1,se);
   C2(closeBW1==1) = 'Rutting';


   BW1 = zeros(rows, columns, 1, 'logical');
```

```
    BW1(C=='Washboarding') = 1;

    BW1 = bwareaopen(BW1,400);

    se = strel('disk', 15);

    closeBW1 = imclose(BW1,se);

    C2(closeBW1==1) = 'Washboarding';



    BW1 = zeros(rows, columns, 1, 'logical');

    BW1(C=='Other') = 1;

    BW1 = bwareaopen(BW1,900);

    se = strel('disk', 15);

    closeBW1 = imclose(BW1,se);

    C2(closeBW1==1) = 'Other';



   B = labeloverlay(I,C2,'Colormap',cmap1,'Transparency',0.6);

   imwrite(B, ['…\Distress_morphological_A2\A2_' num2str(j) '.jpg']);

end
```

Pothole distribution over the road surface – MATLAB Code

```
close all, clear all, clc;

load("…\Test Images\gTruth_1.mat");
imdsTest = imageDatastore('…\Test images\Images');
pxdsTest = pixelLabelDatastore(gTruth);
classes = pxdsTest.ClassNames;


data = load('…\Classifiers\1000\mobilenetv2.mat');
net = data.net;

Headings = {'Estimate'; 'GTruth'};
big_table = table(Headings);
filename = '…\Test Images\PotholeDistribution_mobilenetv2_1000_W.xlsx';

for j=1:119
   my_field = strcat('Image ',num2str(j));
   I = readimage(imdsTest, j);
   C = semanticseg(I, net);

   [rows, columns, Channels] = size(I);
```

```
    BW1 = zeros(rows, columns, 1, 'logical');
    BW1(C=='Other') = 1;
    se = strel('disk', 20);
    closeBW1 = imclose(BW1,se);
    closeBW1 = bwareaopen(closeBW1, 600);

    num_pix_other = sum(closeBW1(:) == 1);
    num_pix_total = numel( closeBW1 );
    num_pix_road = (num_pix_total - num_pix_other);


    BW2 = zeros(rows, columns, 1, 'logical');
    BW2(C=='Potholes') = 1;
    se = strel('disk', 20);
    closeBW2 = imclose(BW2, se);
    closeBW2 = bwareaopen(closeBW2, 600);

    num_pix_pothole = sum(closeBW2(:) == 1);
    pothole_dist = round((num_pix_pothole/num_pix_road)*100, 2);


    expectedResult = readimage(pxdsTest, j);
    BW2 = zeros(rows, columns, 1, 'logical');
    BW2(expectedResult =='Other') = 1;

    num_pix_other = sum(BW2(:) == 1);
    num_pix_Groad = (num_pix_total - num_pix_other);

    BW2 = zeros(rows, columns, 1, 'logical');
    BW2(expectedResult =='Potholes') = 1;
    num_pix_Gpothole = sum(BW2(:) == 1);

    Gpothole_dist = round((num_pix_Gpothole/num_pix_Groad)*100, 2);

    outcome = {pothole_dist; Gpothole_dist};
    T = table(outcome);
    T.Properties.VariableNames = {my_field};
     big_table = [big_table T];
     j
end

  writetable(big_table ,filename,'Sheet',1,'Range','B2');
```